*Inorg. Chem.* **2006**, *45*, 9032–9045


# Chemistry Surrounding Monomeric Copper(I) Methyl, Phenyl, Anilido, Ethoxide, and Phenoxide Complexes Supported by *N*-Heterocyclic Carbene Ligands: Reactivity Consistent with Both Early and Late Transition Metal Systems

**Laurel A. Goj,[†] Elizabeth D. Blue,[†] Samuel A. Delp,[†] T. Brent Gunnoe,*[,†] Thomas R. Cundari,[§] Aaron W. Pierpont,[§] Jeffrey L. Petersen,[‡] and Paul D. Boyle[†]**

*Department of Chemistry, North Carolina State University, Raleigh, North Carolina 27695-8204, C. Eugene Bennett Department of Chemistry, West Virginia University, Morgantown, West Virginia 26506-6045, and Center for Advanced Scientific Computing and Modeling (CASCaM), Department of Chemistry, University of North Texas, Box 305070, Denton, Texas 76203-5070*

Received June 30, 2006

Monomeric copper(I) alkyl complexes that possess the *N*-heterocyclic carbene (NHC) ligands IPr, SIPr, and IMes [IPr = 1,3-bis(2,6-diisopropylphenyl)imidazol-2-ylidene, SIPr = 1,3-bis(2,6-diisopropylphenyl)imidazolin-2-ylidene, IMes = 1,3-bis(2,4,6-trimethylphenyl)imidazol-2-ylidene] react with amines or alcohols to release alkane and form the corresponding monomeric copper(I) amido, alkoxide, or aryloxide complexes. Thermal decomposition reactions of (NHC)Cu$^{I}$ methyl complexes at temperatures between 100 and 130 °C produce methane, ethane, and ethylene. The reactions of (NHC)Cu(NHPh) complexes with bromoethane reveal increasing nucleophilic reactivity at the anilido ligand in the order (SIPr)Cu(NHPh) < (IPr)Cu(NHPh) < (IMes)Cu(NHPh) < (dtbpe)Cu(NHPh) [dtbpe = 1,2-bis(di-*tert*-butylphosphino)ethane]. DFT calculations suggest that the HOMO for the series of Cu anilido complexes is localized primarily on the amido nitrogen with some $p\pi_{anilido}$–$d\pi_{Cu}$ $\pi^*$-character. $[(IPr)Cu(\mu\text{-}H)]_2$ and (IPr)Cu(Ph) react with aniline to quantitatively produce (IPr)Cu(NHPh)/dihydrogen and (IPr)Cu(NHPh)/benzene, respectively. Analysis of the DFT calculations reveals that the conversion of $[(IPr)Cu(\mu\text{-}H)]_2$ and aniline to (IPr)Cu(NHPh) and dihydrogen is favorable with $\Delta H \approx -7$ kcal/mol and $\Delta G \approx -9$ kcal/mol.

## Introduction

The study of transition metal complexes with high d-electron counts that possess nondative heteroaromatic ligands (e.g., amido, alkoxide, imido, oxo, etc.) has substantially increased in the past decade.[1,2] Interest in such systems is derived, in part, from the disruption of ligand-to-metal $\pi$-donation that results from filled d$\pi$-manifolds. Nondative heteroatomic ligands coordinated to transition metals in high oxidation states can $\pi$-donate and form metal−ligand multiple bonds, which can render the nondative ligands relatively inert. In contrast, coordination of nondative heteroatomic ligands to transition metals in low oxidation states disrupts ligand-to-metal $\pi$-donation and often imparts highly nucleophilic and basic character to the nondative ligand.[3−13] For example, late transition metal systems with nondative heteroaromatic ligands have been used for catalytic aryl

* To whom correspondence should be addressed. E-mail: brent_gunnoe@ncsu.edu.
[†] North Carolina State University.
[‡] West Virginia University.
[§] University of North Texas.

(1) Fulton, J. R.; Holland, A. W.; Fox, D. J.; Bergman, R. G. *Acc. Chem. Res.* **2002**, *35*, 44−56.
(2) Sharp, P. R. *Comments Inorg. Chem.* **1999**, *21*, 85−114.
(3) Conner, D.; Jayaprakash, K. N.; Wells, M. B.; Manzer, S.; Gunnoe, T. B.; Boyle, P. D. *Inorg. Chem.* **2003**, *42*, 4759−4772.
(4) Zhang, J.; Gunnoe, T. B.; Petersen, J. L. *Inorg. Chem.* **2005**, *44*, 2895−2907.
(5) Conner, D.; Jayaprakash, K. N.; Cundari, T. R.; Gunnoe, T. B. *Organometallics* **2004**, *23*, 2724−2733.
(6) Fox, D. J.; Bergman, R. G. *J. Am. Chem. Soc.* **2003**, *125*, 8984−8985.
(7) Fulton, J. R.; Sklenak, S.; Bouwkamp, M. W.; Bergman, R. G. *J. Am. Chem. Soc.* **2002**, *124*, 4722−4737.
(8) Zhang, X.-X.; Sadighi, J. P.; Mackewitz, T. W.; Buchwald, S. L. *J. Am. Chem. Soc.* **2000**, *122*, 7606−7607.
(9) Bryndza, H. E.; Tam, W. *Chem. Rev.* **1988**, *88*, 1163−1188.
(10) Mayer, J. M. *Acc. Chem. Res.* **1998**, *31*, 441−450.
(11) Caulton, K. G. *New J. Chem.* **1994**, *18*, 25−41.
(12) Fryzuk, M. D.; Montgomery, C. D. *Coord. Chem. Rev.* **1989**, *95*, 1−40.
(13) Bergman, R. G. *Polyhedron* **1995**, *14*, 3227−3237.



10.1021/ic0611995 CCC: $33.50 
Published on Web 09/27/2006

amination,[14,15] metal-mediated H−H and C−H bond activation,[5,16−20] heterolytic cleavage of C−H bonds,[3,7,21−25] polymerization of anilines, $\beta$-lactams, and carbodiimides,[8,26,27] catalytic hydration of nitriles,[28,29] stoichiometric N−C and O−C bond formation,[4,13,24,25,30,31] and access to low-coordination numbers and high-spin states (in some cases) with imido or oxo ligands.[32−38]

On the basis of a $d^{10}$ electron count (i.e., filled d$\pi$-orbital set) and metal-based Lewis acidity, it might be anticipated that $Cu^{I}$ complexes with amido, alkoxide, and related ligands would be highly reactive; however, the potential for increased covalent character for the Cu−X bonds (compared with earlier transition metals) may serve to attenuate reactivity at the nondative ligand. According to several scales, elemental Cu possesses substantial electronegativity relative to other transition metals;[39] however, although elemental Cu is more electronegative than elemental Ru by most scales, $Cu^{I}$ is reported to be less electronegative than $Ru^{II}$ using the Pauling scale for electronegativity (1.9 vs 2.2).[40] With the latter electronegativities, a more polar metal−ligand bond is expected for $Cu^{I}$ compared with that of $Ru^{II}$, a prediction that is counter to general trends in electronegativity. Hence, the effects of formal oxidation states complicate any comparisons between transition metal complexes that are based on electronegativity differences.

**Chart 1.** *N*-Heterocyclic Carbene Ligands Used to Form $Cu^{I}$ Systems and Generic Depiction of the NHC Ligands

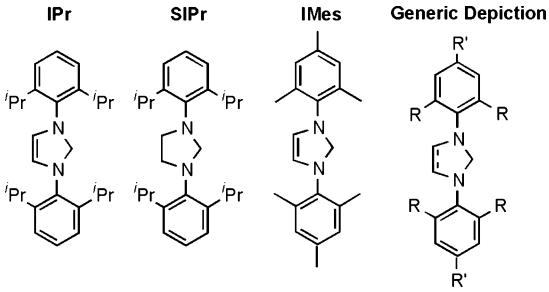


Examples of monomeric and well-defined copper complexes with alkyl, aryl, amido, alkoxide, and aryloxide ligands are relatively uncommon. Sadighi et al. have recently reported the isolation and reactivity of a unique two-coordinate $Cu^{I}$ methyl complex with a *N*-heterocyclic carbene (NHC) supporting ligation.[41] Although more common than alkyl complexes, structurally characterized monomeric $Cu^{I}$ alkoxides are also quite limited.[42−44] To our knowledge, the isolation of monomeric $Cu^{I}$ amido complexes is extremely rare.[45,46]

We recently communicated that the reactions of substrates that possess N−H, O−H, and acidic C−H bonds with $Cu^{I}$ alkyl complexes with the NHC ligand IPr {IPr = 1,3-bis-(2,6-diisopropylphenyl)imidazol-2-ylidene} produce *monomeric* $Cu^{I}$ anilido, ethoxide, phenoxide, phenylacetylide, and *N*-pyrrolyl complexes, which serve as catalysts for the anti-Markovnikov addition of amines and alcohols to electron-deficient olefins.[46−47] Herein, we report the synthesis and characterization of a series of $Cu^{I}$ methyl, phenyl, anilido, ethoxide, and phenoxide complexes with the NHC ligands IPr, IMes [IMes = 1,3-bis(2,4,6-trimethylphenyl)imidazol-2-ylidene], and SIPr [SIPr = 1,3-bis(2,6-diisopropylphenyl)-imidazolin-2-ylidene], including details of characterization, solid-state structures, comparative reactivity studies, and DFT calculations relevant to the observed reactivity.

## Results and Discussion

**Synthesis and Characterization of $Cu^{I}$ Methyl and Phenyl Complexes.** Herein, we report a series of monomeric copper (I) methyl, phenyl, anilido, ethoxide, and phenoxide complexes that have been formed using three different NHC ligands (Chart 1). Sadighi et al. previously reported the synthesis of (IPr)Cu(Me) (**1**) from (IPr)Cu(OAc) and tri-

(14) Hartwig, J. F. *Angew. Chem., Int. Ed.* **1998**, *37*, 2046−2067.
(15) Wolfe, J. P.; Wagaw, S.; Marcoux, J.-F.; Buchwald, S. L. *Acc. Chem. Res.* **1998**, *31*, 805−818.
(16) Feng, Y.; Lail, M.; Barakat, K. A.; Cundari, T. R.; Gunnoe, T. B.; Petersen, J. L. *J. Am. Chem. Soc.* **2005**, *127*, 14174−14175.
(17) Feng, Y.; Lail, M.; Foley, N. A.; Gunnoe, T. B.; Barakat, K. A.; Cundari, T. R.; Petersen, J. L. *J. Am. Chem. Soc.* **2006**, *128*, 7982−7994.
(18) Tenn, W. J., III; Young, K. J. H.; Bhalla, G.; Oxgaard, J.; Goddard, W. A., III; Periana, R. A. *J. Am. Chem. Soc.* **2005**, *127*, 14172−14173.
(19) Abdur-Rashid, K.; Faatz, M.; Lough, A. J.; Morris, R. H. *J. Am. Chem. Soc.* **2001**, *123*, 7473−7474.
(20) Fryzuk, M. D.; Montgomery, C. D.; Rettig, S. J. *Organometallics* **1991**, *10*, 467−473.
(21) Jayaprakash, K. N.; Conner, D.; Gunnoe, T. B. *Organometallics* **2001**, *20*, 5254−5256.
(22) Conner, D.; Jayaprakash, K. N.; Gunnoe, T. B.; Boyle, P. D. *Inorg. Chem.* **2002**, *41*, 3042−3049.
(23) Fulton, J. R.; Bouwkamp, M. W.; Bergman, R. G. *J. Am. Chem. Soc.* **2000**, *122*, 8799−8800.
(24) Fox, D. J.; Bergman, R. G. *Organometallics* **2004**, *23*, 1656−1670.
(25) Holland, A. W.; Bergman, R. G. *J. Am. Chem. Soc.* **2002**, *124*, 14684−14695.
(26) Cheng, J.; Deming, T. J. *J. Am. Chem. Soc.* **2001**, *123*, 9457−9458.
(27) Shibayama, K.; Seidel, S. W.; Novak, B. M. *Macromolecules* **1997**, *30*, 3159−3163.
(28) Breno, K. L.; Pluth, M. D.; Tyler, D. R. *Organometallics* **2003**, *22*, 1203−1211.
(29) Kian, J. H.; Britten, J.; Chin, J. *J. Am. Chem. Soc.* **1993**, *115*, 3618−3622.
(30) Zhang, J.; Gunnoe, T. B.; Boyle, P. D. *Organometallics* **2004**, *23*, 3094−3097.
(31) Rais, D.; Bergman, R. G. *Chem.−Eur. J.* **2004**, *10*, 3970−3978.
(32) Dai, X.; Kapoor, P.; Warren, T. H. *J. Am. Chem. Soc.* **2004**, *126*, 4798−4799.
(33) Kogut, E.; Wiencko, H. L.; Zhang, L.; Cordeau, D. E.; Warren, T. H. *J. Am. Chem. Soc.* **2005**, *127*, 11248−11249.
(34) Mehn, M. P.; Peters, J. C. *J. Inorg. Biochem.* **2006**, *100*, 634−643.
(35) Brown, S. D.; Peters, J. C. *J. Am. Chem. Soc.* **2005**, *127*, 1913−1923.
(36) Thyagarajan, S.; Shay, D. T.; Incarvito, C. D.; Rheingold, A. L.; Theopold, K. H. *J. Am. Chem. Soc.* **2003**, *125*, 4440−4441.
(37) Shay, D. T.; Yap, G. P. A.; Zakharov, L. N.; Rheingold, A. L.; Theopold, K. H. *Angew. Chem., Int. Ed.* **2005**, *44*, 1508−1510.
(38) Eckert, N. A.; Stoian, S.; Smith, J. M.; Bominaar, E. L.; Muenck, E.; Holland, P. L. *J. Am. Chem. Soc.* **2005**, *127*, 9344−9345.
(39) Mann, J. B.; Meek, T. L.; Knight, E. T.; Capitani, J. F.; Allen, L. C. *J. Am. Chem. Soc.* **2000**, *122*, 5132−5137.
(40) Allred, A. L. *J. Inorg. Nucl. Chem.* **1961**, *17*, 215−221.
(41) Mankad, N. P.; Gray, T. G.; Laitar, D. S.; Sadighi, J. P. *Organometallics* **2004**, *23*, 1191−1193.
(42) Mankad, N. P.; Laitar, D. S.; Sadighi, J. P. *Organometallics* **2004**, *23*, 3369−3371.
(43) Purdy, A. P.; George, C. F.; Callahan, J. H. *Inorg. Chem.* **1991**, *30*, 2812−2819.
(44) Osakada, K.; Takizawa, T.; Tanaka, M.; Yamamoto, T. *J. Organomet. Chem.* **1994**, *473*, 359−369.
(45) Blue, E. D.; Davis, A.; Conner, D.; Gunnoe, T. B.; Boyle, P. D.; White, P. S. *J. Am. Chem. Soc.* **2003**, *125*, 9435−9441.
(46) Goj, L. A.; Blue, E. D.; Munro-Leighton, C.; Gunnoe, T. B.; Petersen, J. L. *Inorg. Chem.* **2005**, *44*, 8647−8649.
(47) Munro-Leighton, C.; Blue, E. D.; Gunnoe, T. B. *J. Am. Chem. Soc.* **2006**, *128*, 1446−1447.

**Scheme 1.** Reaction of (NHC)Cu(Me) Complexes with Aniline, Ethanol, or Phenol to Produce the Corresponding (NHC)Cu(X) (X = anilido, ethoxide, or phenoxide) Complexes

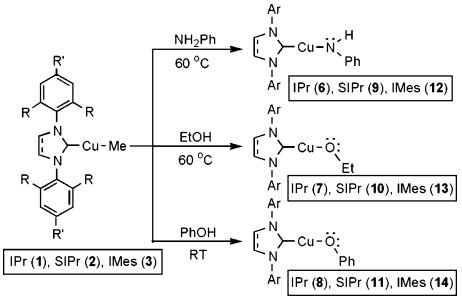


methylaluminum.[42] We used the same methodology to synthesize the analogous monomeric Cu$^{I}$ complexes (SIPr)Cu(Me) (**2**) and (IMes)Cu(Me) (**3**) (eq 1).

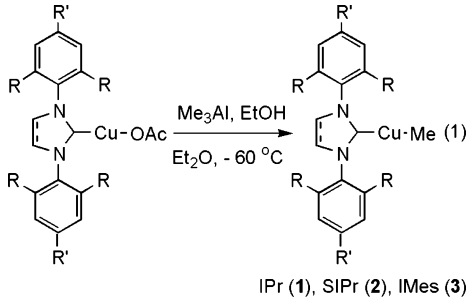


In addition, complex **3** is cleanly produced upon reaction of (IMes)Cu(Cl) and MeLi. The phenyl complexes, (IPr)Cu(Ph) (**4**) and (SIPr)Cu(Ph) (**5**), are formed from the reaction of the corresponding (NHC)Cu(Cl) complex and $Ph_2Mg$ (eq 2).

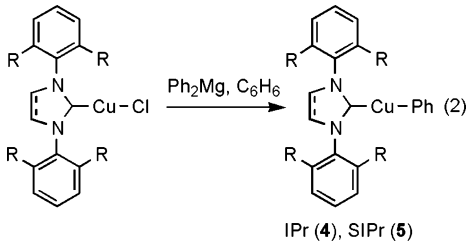


$^1$H NMR spectroscopy reveals that **5** is formed with a minor intractable impurity in an approximately 4:1 ratio. Although the NMR spectra reveal pure material, we were not able to obtain satisfactory elemental analysis of the phenyl complex **4**. Similar difficulties have been reported for the (NHC)Cu(Me) systems.[42,48]

**Synthesis and Characterization of Cu$^{I}$ Anilido, Ethoxide, and Phenoxide Complexes.** Recently, we reported the syntheses and characterization of (IPr)Cu(NHPh) (**6**), (IPr)Cu(OEt) (**7**), and (IPr)Cu(OPh) (**8**) upon reaction of complex **1** with aniline, ethanol, and phenol, respectively.[46] Similar procedures were used to prepare and isolate the series of complexes (SIPr)Cu(X) [X = NHPh (**9**), OEt (**10**), and OPh (**11**)] and (IMes)Cu(X) [X = NHPh (**12**), OEt (**13**), and OPh (**14**)] (Scheme 1). In addition, the anilido complexes can be synthesized by metathesis of (NHC)Cu(Cl) with LiNHPh.[46] Complex (IMes)Cu(OEt) (**13**) could not be isolated in the solid-state and is only stable in solution in the presence of a slight excess of free EtOH (see Experimental Section for details).

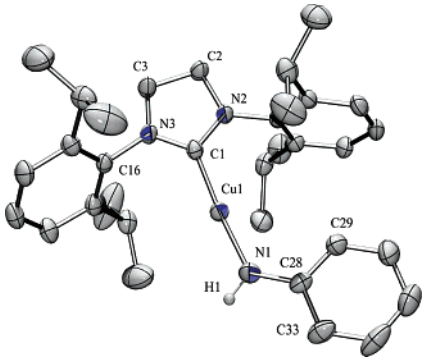


**Figure 1.** ORTEP of (SIPr)Cu(NHPh) (**9**) at 30% probability (selected hydrogen atoms omitted). Selected bond distances (Å): C2−C3 = 1.517(3), N3−C1 = 1.334(2), N2−C1 = 1.347(2), Cu1−C1 = 1.876(2), Cu1−N1 = 1.846(2), N1−C28 = 1.359(3). Selected bond angles (deg): N2−C1−Cu1 = 121.9(1), N3−C1−Cu1 = 130.8(1), C1−Cu1−N1 = 175.21(7), Cu1−N1−C28 = 127.9(1), N2−C1−N3 = 107.2(2).

**Solid-State Structures of Cu$^{I}$ Anilido Complexes.** The solid-state structures of **6** and (dtbpe)Cu(NHPh) [dtbpe = 1,2-bis(di-*tert*-butylphosphino)ethane] have been reported.[45,46] Single-crystals of **9** suitable for X-ray diffraction (XRD) study were obtained to compare the structures of the copper anilido complexes. Figure 1 depicts an ORTEP of **9**, and Table 1 provides crystallographic data and collection parameters for all structures reported herein. Both (NHC)Cu(NHPh) complexes **6** and **9** exhibit a linear geometry with C1−Cu1−N1 bond angles of approximately 175°. The plane of the anilido phenyl is approximately coplanar with the H−N−$C_{phenyl}$ plane, which optimizes delocalization of the amido lone pair into the phenyl $\pi$*-system (see discussion below). This geometric feature is consistent for all three Cu$^{I}$ anilido complexes (Figure 2). The Cu1−N1 bond distances of complexes **6** and **9** are statistically identical at 1.841(2) and 1.846(2) Å, respectively. Thus, the saturated backbone of the SIPr ligand, compared with the unsaturated IPr backbone, does not appear to substantially impact Cu−$N_{amido}$ bonding. The Cu−$N_{amido}$ bond distances are also shorter than, but comparable to, the Cu−$N_{amido}$ bond distance of 1.890(6) Å for (dtbpe)Cu(NHPh).[45,46] The $N_{amido}$−$C_{ipso}$ bond distances of complexes **6**, **9**, and (dtbpe)Cu(NHPh) are statistically identical at 1.351(4), 1.359(3), and 1.354(9) Å, respectively. These bond distances are shorter than a typical N−C single bond (~1.47 Å) and the corresponding bond distance of the amine complex [(dtbpe)Cu($NH_2$Ph)][$PF_6$], which is 1.444(4) Å.[45] Thus, the solid-state $N_{amido}$−$C_{ipso}$ bond distances of the Cu$^{I}$ anilido complexes are consistent with some N−C multiple bonding.

**Variable-Temperature NMR of (IPr)Cu(NHPh) (6).** The ability of the aryl $\pi$*-system to delocalize electron density from the amido lone pair is likely a contributing factor for the relatively high abundance of aryl amido complexes, compared with that of the parent and alkyl amido systems. Hindered bond rotations about the $N_{amido}$−$C_{ipso}$

(48) Goj, L. A.; Blue, E. D.; Delp, S. A.; Gunnoe, T. B.; Cundari, T. R.; Petersen, J. L. *Organometallics* **2006**, *25*, 4097−4104.

**Figure 2.** Depiction of orientation of phenyl substituents of anilido ligands of (SIPr)Cu(NHPh) (**9**) (left), (IPr)Cu(NHPh) (**6**) (middle), and (dtbpe)Cu(NHPh) (right) with most atoms removed (carbon and hydrogen are gray, nitrogen is blue, copper is orange, and phosphorus is pink). The structures of the latter two complexes have been previously reported.[45,46]

**Table 1.** Selected Crystallographic Data and Collection Parameters for Complexes (SIPr)Cu(NHPh) (**9**), (SIPr)Cu(OEt) (**10**), (SIPr)Cu(OPh) (**11**), and (IMes)Cu(OPh) (**14**)

| | **9** | **10** | **11** | **14** |
|---|---|---|---|---|
| empirical formula | $C_{33}H_{44}CuN_3$ | $C_{29}H_{43}CuN_2O$ | $C_{38.25}H_{49}CuN_2O$ | $C_{30}H_{25}CuN_2O$ |
| fw | 546.25 | 499.19 | 616.33 | 500.14 |
| cryst syst | orthorhombic | monoclinic | triclinic | monoclinic |
| space group | $P2_12_12_1$ | $Cc$ | $P\bar{1}$ | $C2/c$ |
| $a$ (Å) | 11.932(1) | 17.434(3) | 12.115(2) | 16.8260(9) |
| $b$ (Å) | 12.545(1) | 12.791(2) | 14.279(2) | 23.1927(1) |
| $c$ (Å) | 20.706(2) | 13.284(2) | 22.971(4) | 15.4484(1) |
| α (deg) | | | 77.627(3) | |
| $\beta$ (deg) | 90.0 | 93.200(4) | 86.060(3) | 120.164(2) |
| $\gamma$ (deg) | | | 71.445(3) | |
| $V$ (Å$^3$) | 3099.3(4) | 2957.6(9) | 3680(1) | 5212.3(6) |
| $Z$ | 4 | 4 | 4 | 8 |
| $D_{calcd}$ (g cm$^{-3}$) | 1.171 | 1.121 | 1.113 | 1.275 |
| cryst size (mm) | 0.15 × 0.20 × 0.50 | 0.16 × 0.22 × 0.30 | 0.14 × 0.20 × 0.40 | 0.30 × 0.27 × 0.07 |
| R1, wR2 {I>2$\sigma$(I)}[a] | 0.0408, 0.0931 | 0.0649, 0.1311 | 0.0677, 0.1455 | 0.044, 0.056 |
| GOF[a] | 1.019 | 0.924 | 0.716 | 1.75 |

[a] For definitions of wR2 and GOF see Supporting Information.

bonds of the aryl amido complexes have been observed,[22,49−51] and partial $N_{amido}-C_{ipso}$ multiple bonding caused by electron delocalization may contribute in some cases to the activation barriers for N−C bond rotation. Support for this delocalization can also be found in the DFT-optimized geometries of NHC−Cu−anilido (NHC = IPr, SIPr, and IMes), which revealed calculated $N_{amido}-C_{ipso}$ bond distances of 1.38 Å, or approximately 0.04 Å shorter than aniline-optimized at the same level of theory, as well as the experimental $N_{amido}-C_{ipso}$ bond distances of ∼1.35 Å (see above). Variable-temperature $^1$H NMR spectroscopy in toluene-$d_8$ (22 to −80 °C) was used to study the dynamics of complex **6**. At room temperature, a single time-averaged resonance is observed because of the ortho position of the amido phenyl. At reduced temperatures, this resonance broadens and decoalesces into two doublets, which resonate at 6.26 and 5.33 ppm in the slow-exchange regime, which is accessed at −70 °C. The observed changes are consistent with slow rotation (at lower temperatures) about the $N_{amido}-C_{ipso}$ bond relative to the NMR time scale. No evidence for slow rotation (on the NMR time scale) about the $Cu-N_{amido}$ bond is observed at temperatures down to −80 °C. The rate of $N_{amido}-C_{ipso}$ bond rotation has been calculated at the coalescence temperature (−40 °C, $k = 6.4 \times 10^2$ s$^{-1}$) and in the fast-exchange regime using line broadening. Table 2 depicts rate constants and calculated $\Delta G^{\ddagger}$ values. An Eyring plot of these data reveals $\Delta H^{\ddagger} = 7$ kcal/mol and $\Delta S^{\ddagger} = -14$ eu (Figure 3).

**Table 2.** Rate Constants and Calculated Gibbs Free Energy of Activation for Rotation about $N_{Amido}-C_{Ipso}$ Bond of (IPr)Cu(NHPh) (**6**)

| temp (°C) | $k$ (s$^{-1}$) | $\Delta G^{\ddagger}$ (kcal/mol) |
|---|---|---|
| 0 | $8.7 \times 10^3$ | 11.0 |
| −10 | $2.9 \times 10^3$ | 11.2 |
| −20 | $1.5 \times 10^3$ | 11.0 |
| −40 | $6.4 \times 10^2$ | 10.5 |

**Solid-State Structures of Cu$^I$ Ethoxide and Phenoxide Complexes.** We have previously reported details of the solid-state structure of (IPr)Cu(OEt) (**7**).[46] Single-crystals of **10** suitable for an XRD study were obtained (Figure 4). Both (NHC)Cu(OEt) complexes **7** and **10** exhibit a nearly linear geometry with C1−Cu1−O1 bond angles of approximately 176°. The Cu1−O1 bond distances of complexes **7** and **10** are statistically identical at 1.799(3) and 1.793(7) Å, respectively.[46] The solid-state structures of two monomeric Cu$^I$ alkoxide complexes have been reported. The Cu−O bond lengths for $Cu\{OCH(CF_3)_2\}(PPh_3)$ and (IPr)Cu(O$^t$Bu) are 2.087(6) and 1.8104(13) Å, respectively.[42,44] The longer bond distance of $Cu\{OCH(CF_3)_2\}(PPh_3)$ is likely a result of the electron-withdrawing perfluoromethyl groups.

The solid-state structure of (IPr)Cu(OPh) (**8**) has been previously reported,[46] and herein, we report the structures of complexes **11** and **14** (Figures 5 and 6). Complex **11** contained two independent molecules in the crystallographic asymmetric cell. All three copper phenoxide complexes exhibit a linear geometry with C1−Cu1−O1 bond angles ranging from 173° to 178°. The Cu1−O1 bond distances of complexes **8**, **11**, and **14** are similar at 1.839(2), 1.831(3), and 1.833(1) Å, respectively.[46] These bond distances are shorter than the Cu−O bond length of 1.917(3) Å reported for the complex $[(p\text{-}MeC_6H_4NC)_2Cu(2,6\text{-}^tBu_2C_6H_3O)]$.[52]

(49) Powell, K. R.; Pérez, P. J.; Luan, L.; Feng, S. G.; White, P. S.; Brookhart, M.; Templeton, J. L. *Organometallics* **1994**, *13*, 1851−1864.
(50) Albéniz, A. C.; Calle, V.; Espinet, P.; Gómez, S. *Inorg. Chem.* **2001**, *40*, 4211−4216 and references therein.
(51) Jayaprakash, K. N.; Gunnoe, T. B.; Boyle, P. D. *Inorg. Chem.* **2001**, *40*, 6481−6486.

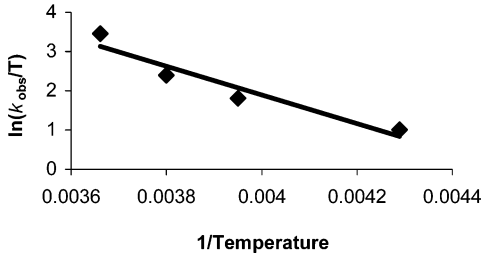


**Figure 3.** Eyring plot for $N_{amido}-C_{ipso}$ bond rotation of (IPr)Cu(NHPh) (**6**) ($R^2 = 0.92$).

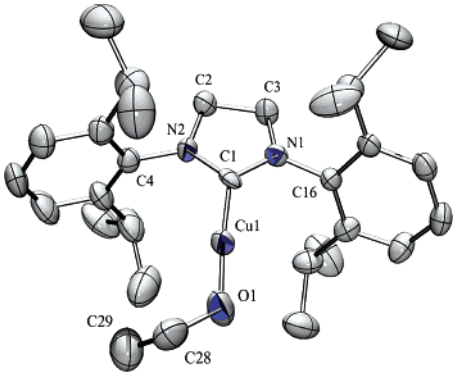


**Figure 4.** ORTEP of (SIPr)Cu(OEt) (**10**) at 30% probability (hydrogen atoms omitted). Selected bond distances (Å): C2−C3 = 1.531(9), N1−C1 = 1.321(8), N2−C1 = 1.353(8), Cu1−C1 = 1.861(8), Cu1−O1 = 1.793-(7), O1−C28 = 1.31(1), C28−C29 = 1.49(1). Selected bond angles (deg): N1−C1−Cu1 = 128.0(5), N2−C1−Cu1 = 124.6(5), C1−Cu1−O1 = 175.9(4), Cu1−O1−C28 = 123.3(6), N1−C1−N2 = 107.4(6).

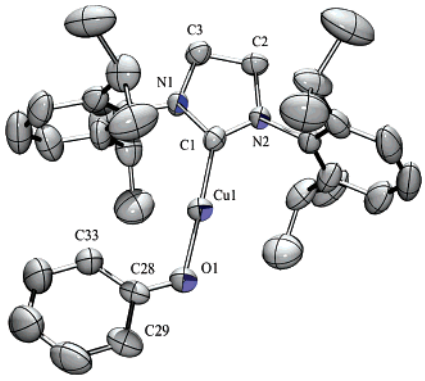


**Figure 5.** ORTEP of one of two independent molecules of (SIPr)Cu-(OPh) (**11**) at 30% probability (hydrogen atoms omitted). Selected bond distances (Å): C2−C3 = 1.520(5), N1−C1 = 1.341(5), N2−C1 = 1.322-(5), Cu1−C1 = 1.881(4), Cu1−O1 = 1.831(3), O1−C28 = 1.302(5). Selected bond angles (deg): N1−C1−Cu1 = 122.6(3), N2−C1−Cu1 = 128.1(3), C1−Cu1−O1 = 178.3(2), Cu1−O1−C28 = 121.5(3), N1−C1−N2 = 109.3(4).

The effect of the identity of the nondative ligand on the trans $Cu-C_{NHC}$ bond length of (NHC)Cu(X) (X = Me, NHPh, OEt, or OPh) systems was examined (Table 3). The $Cu-C_{IPr}$ bond distance decreases in the order Me > NHPh > OEt ≈ OPh. As the electronegativity of the nondative ligand increases and its $\sigma$-donor ability presumably decreases, the trans $Cu-C_{NHC}$ bond distance decreases.

**Thermal Decomposition of $Cu^{I}$ Methyl and Phenyl Complexes.** Solutions of **1**, **2**, and **3** in $C_6D_6$ were heated to temperatures between 100 and 130 °C and monitored by $^1H$ NMR spectroscopy (Scheme 2). Visual inspection of the NMR tubes indicated decomposition of the copper complexes in the form of a black precipitate or pink plating and a concomitant change in solution from colorless to pale yellow. The $^1H$ NMR spectra reveal the formation of several uncharacterized (NHC)Cu systems without the formation of free or protonated NHC ligands. In addition, three new singlets at 0.16, 0.80, and 5.26 ppm are observed, which are consistent with the resonances for methane, ethane, and ethylene, respectively. The resonance from methane is a singlet, which is consistent with the formation of $CH_4$ rather than $CH_3D$. Mass spectrometry was used to analyze the headspace of the reaction mixture from the thermolysis of complex **2**, and the data confirm the formation of methane, ethane, and ethylene. Similar to the methyl complexes **1**−**3**, heating of the $C_6D_6$ solutions of the phenyl complexes **4** and **5** to 120 and 130 °C, respectively, results in decomposition; however, unambiguous identification of the products (organic or organometallic) was not possible.

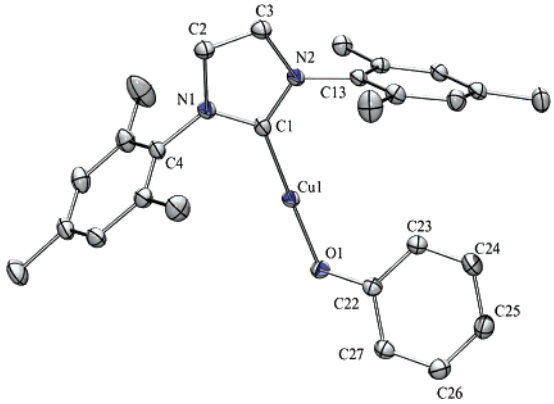


**Figure 6.** ORTEP of (IMes)Cu(OPh) (**14**) at 30% probability (hydrogen atoms omitted). Selected bond distances (Å): C2−C3 = 1.352(2), N1−C1 = 1.354(2), N2−C1 = 1.366(2), Cu1−C1 = 1.864(2), Cu1−O1 = 1.833-(1), O1−C22 = 1.344(2). Selected bond angles (deg): N1−C1−Cu1 = 130.2(1), N2−C1−Cu1 = 125.5(1), C1−Cu1−O1 = 175.53(6), Cu1−O1−C22 = 117.36(6).

**Table 3.** $Cu-C_{NHC}$ Bond Distances (Å) of (NHC)Cu(X) (NHC = IPr or SIPr; X = NHPh, OEt, or OPh) as a Function of the Identity of X[a]

| X | $Cu-C_{IPr}$ (Å) | $Cu-C_{SIPr}$ (Å) |
|---|---|---|
| Me | 1.887(5) | |
| NHPh | 1.875(3) | 1.876(2) |
| OEt | 1.863(5) | 1.861(8) |
| OPh | 1.868(2) | 1.881(4) |

[a] Solid-state structures of (IPr)Cu(Me) and (IPr)Cu(X) have been previously reported.[42,46]

**Scheme 2.** Thermal Decomposition of (NHC)Cu(Me) Complexes **1**−**3**

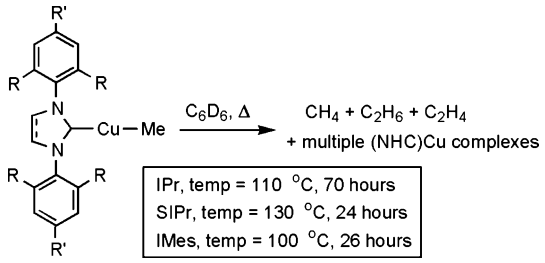


(52) Fiaschi, P.; Floriani, C.; Pasquali, M.; Chiesa-Villa, A.; Guastini, C. *J. Chem. Soc., Chem. Commun.* **1984**, 888−890.

**Scheme 3.** Calculated Free Energy Changes (kcal/mol) for C−H Activation of Benzene by (SIPr)Cu(Me) (**2**) and (SIPr)Cu(Ph) (**5**)

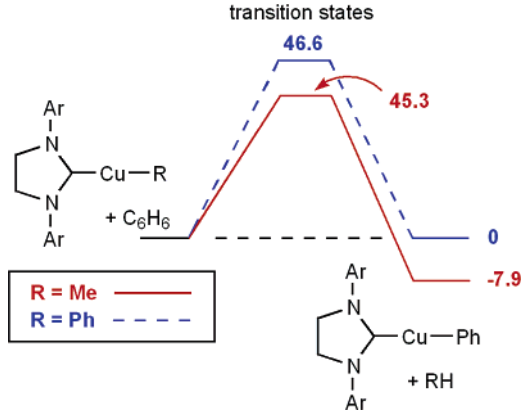


One potential pathway for the formation of the organic products from (NHC)Cu(Me) is the initial bond homolysis of the Cu−Me linkage leading to the transient formation of a methyl radical. The heating of solutions of **2** in $C_6D_6$ in the presence of TEMPO (2,2,6,6-tetramethylpiperidinyloxy) or 1,4-cyclohexadiene leads to the formation of methane, ethane, and ethylene without additional organic products that would result from trapping of the methyl radical by TEMPO or 1,4-cyclohexadiene. Furthermore, heating of solutions of **1** or **2** in toluene-$d_8$, which possesses a weak benzylic C−H(D) bond and would be anticipated to yield $CH_3D$ if methyl radical were formed, results in no change from reactions in $C_6D_6$. Thus, the thermal decompositions of **1**−**3** do not likely involve $Cu-C_{Me}$ bond homolysis. The lack of Cu−R bond homolysis, even at elevated temperatures, is consistent with calculated $Cu-C_{Me}$ bond dissociation energies for (NHC)Cu(Me) systems of ∼80 kcal/mol (see below).

We have recently reported evidence that single-electron oxidation of (NHC)Cu(R) (R = Me or Et) complexes to unobserved $Cu^{II}$ cations, $[(NHC)Cu(R)]^+$, results in rapid reductive elimination of alkane "$R_2$" and formation of (NHC)Cu(X).[48] Mechanistic studies suggest that the elimination of $R_2$ from $Cu^{II}$ occurs via a bimolecular pathway that does not involve Cu−C bond homolysis; however, in contrast to the thermal decomposition of $Cu^{I}$ complexes, such as (NHC)Cu(Me), decomposition of the $Cu^{II}$ alkyl complexes does not result in formation of olefins (by $^1$H NMR spectroscopy), and methane formation is negligible from $Cu^{II}$.[48] Thus, the decomposition pathways of (NHC)Cu(R) and $[(NHC)Cu(R)]^+$ appear to be mechanistically distinct, although neither appears to occur through $Cu-C_{alkyl}$ bond homolysis. Unfortunately, attempts to follow the kinetics of the thermal decomposition of (NHC)Cu(Me) systems gave highly varied results. Whitesides et al. have reported that the decomposition of $(Bu_3P)Cu(n\text{-butyl})$ at 0 °C involves initial $\beta$-hydride elimination, followed by reduction of starting material by the resulting Cu−hydride complex,[53] while $[\{PhC(Me)_2CH_2\}Cu(PBu_3)]_n$, which lacks a $\beta$-hydrogen atom, undergoes decomposition at 30 °C with product distributions that are consistent with Cu−C bond homolysis.[54] The (NHC)Cu(Me) systems do not undergo Cu−C bond homolysis nor do they possess $\beta$-hydrogen atoms for an initial $\beta$-hydride elimination step. Thus, the thermal decomposition of (NHC)Cu(Me) complexes likely proceeds by a mechanism that is distinct from those observed for $(Bu_3P)$-Cu(R) systems.

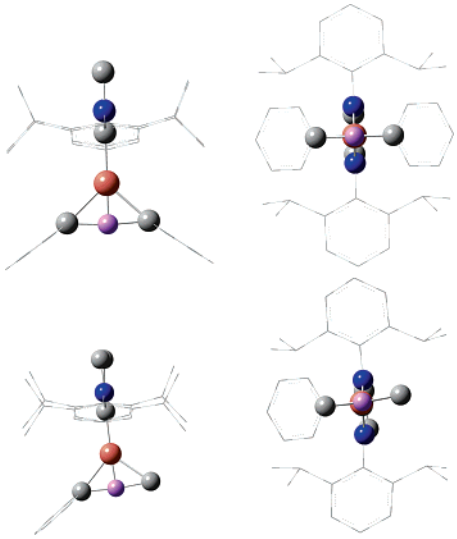

**Figure 7.** B3LYP/6-31G(d) calculated transition states for benzene C−H activation by (SIPr)Cu(Ph) (**5**) (top) and (SIPr)Cu(Me) (**2**) (bottom). Hydrogen atoms are omitted for clarity except for the active hydrogen participating in the metathesis reaction; atoms of the NHC and the active site are shown as spheres with the remainder in wire frame. Views are along the $Cu-C_{NHC}$ axis (right) and perpendicular to this axis (left).

The heating of complexes **1**−**5** in $C_6D_6$ (100 °C to 130 °C) does not lead to activation of benzene C−H(D) bonds to form (NHC)Cu(Ph-$d_5$) and either $CH_3D$ or $C_6H_5D$. DFT calculations on full SIPr models were performed to ascertain the energetics of benzene C−H bond activation by (SIPr)-Cu(Me) (**2**) and (SIPr)Cu(Ph) (**5**) (Scheme 3). We first assessed the potential radical reactivity of (SIPr)Cu(Me) (**2**) and (SIPr)Cu(Ph) (**5**) through calculation of the Cu−C homolytic bond dissociation enthalpies (BDEs) to produce methyl and phenyl radicals, respectively. The B3LYP/6-31G-(d) computations indicate that the Cu−C bonds possess substantial bond strength with $BDE_{Cu-Me}$ = 80 kcal/mol for **2** and $BDE_{Cu-Ph}$ = 95 kcal/mol for **5**. The large Cu−C BDEs are consistent with experimental results that suggest that Cu−C bond homolysis does not occur, even at elevated temperatures.

The thermodynamics and kinetics for benzene C−H bond activation via four-centered $\sigma$-bond metathesis transition states (TS) were also calculated at the B3LYP/6-31G(d) level of theory for full SIPr models. The calculated TSs are shown in Figure 7. Pertinent calculated thermodynamics (in kcal/mol) at STP are $\Delta H_{rxn}$ = −9.1 (Me), 0.0 (Ph) and $\Delta G_{rxn}$ = −7.9 (Me), 0.0 (Ph). The favorable driving force for Me/Ph ligand exchange for complex **2** is consistent with the relative BDEs of Cu−Ph > Cu−Me (by ∼15 kcal/mol), while the difference in the C−H BDE between $CH_4$ and $C_6H_6$ is

(53) Whitesides, G. M.; Stedronsky, E. R.; Casey, C. P.; San Filippo, J., Jr. *J. Am. Chem. Soc.* **1970**, *92*, 1426−1427.

(54) Whitesides, G. M.; Panek, E. J.; Stedronsky, E. R. *J. Am. Chem. Soc.* **1972**, *94*, 232−239.

**Scheme 4.** Nucleophilic Substitution Reaction of Amido Complexes with Bromoethane

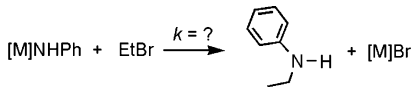


[M] = (dtbpe)Cu, (IPr)Cu (**6**), (SIPr)Cu (**9**), (IMes)Cu (**12**) or $TpRu(PMe_3)_2$

**Table 4.** Kinetic Data for the Reaction of Bromoethane with (IPr)Cu(NHPh) (**6**), (SIPr)Cu(NHPh) (**9**), (IMes)Cu(NHPh) (**12**), (dtbpe)Cu(NHPh), and $TpRu(PMe_3)_2(NHPh)$[a]

| | $k_{obs}$ ($s^{-1}$) | $t_{1/2}$[c] | $\Delta G^{\ddagger}$[d] |
|---|---|---|---|
| (dtbpe)Cu(NHPh) | $5.5(2) \times 10^{-4}$ | 21.0(6) | 21.7 |
| (IMes)Cu(NHPh) (**12**) | $3.3(3) \times 10^{-4}$ | 35(3) | 22.0 |
| (IPr)Cu(NHPh) (**6**) | $2.4(2) \times 10^{-4}$ | 49(4) | 22.2 |
| (SIPr)Cu(NHPh) (**9**) | $1.1(1) \times 10^{-4}$ | 109(8) | 22.6 |
| $TpRu(PMe_3)_2(NHPh)$[b] | $8.6(3) \times 10^{-6}$ | 22[e] | 29.0 |

[a] All reactions at room temperature except $TpRu(PMe_3)_2NHPh$, which was acquired at 80 °C. [b] Reported in ref 45. [c] In minutes. [d] In kilocalories per mole. [e] In hours.

approximately 6 kcal/mol {B3LYP/6-31G(d)-calculated BDE(Me−H) = 104.8 kcal/mol, BDE(Ph−H) = 110.7 kcal/mol}. The calculated activation barriers for benzene C−H activation by **2** and **5** are substantial [transition states relative to separated reactants (SIPr)Cu(R) and benzene] with similar enthalpies, $\Delta H^{\ddagger} = 35.3$ (Me/Ph) and 35.1 (Ph/Ph) kcal/mol. In terms of free energy, there is a more discernible difference between Me/Ph and Ph/Ph metathesis: $\Delta G^{\ddagger} = 45.3$ (Me/Ph) and 46.6 (Ph/Ph) kcal/mol.

**Reactivity of Copper(I) Anilido Complexes with Bromoethane.** We have reported that the anilido complexes $TpRu(PMe_3)_2NHPh$ and (dtbpe)Cu(NHPh) undergo apparent $S_N2$ reactions with bromoethane to produce $TpRu(PMe_3)_2$-Br and (dtbpe)Cu(Br), respectively, as well as ethylaniline.[45] The (NHC)Cu(NHPh) [NHC = IPr (**6**), SIPr (**9**), or IMes (**12**)] systems undergo analogous reactions. To compare the impact of the ancillary ligand on nucleophilic reactivity, kinetic studies were undertaken for the reaction of (IPr)Cu(NHPh) (**6**), (SIPr)Cu(NHPh) (**9**), and (IMes)Cu(NHPh) (**12**) with bromoethane. All three reactions cleanly produce ethylaniline and a (NHC)Cu product with resonances consistent with (NHC)Cu(Br) (Scheme 4). The rates and half-lives of these reactions and those of previously reported complexes are summarized in Table 4.

The copper(I) anilido complexes undergo significantly more rapid reaction with bromoethane than the TpRu anilido complex. For the (NHC)Cu(NHPh) complexes, the reactivity decreases in the order IMes > IPr > SIPr (Chart 2). The difference in rate between **6** and **12** is likely the result of steric effects. For complex **9**, the saturated backbone of the SIPr ligand decreases the rate of the nucleophilic reaction by approximately 2-fold relative to that of the IPr analogue **6**.

We postulated that the increased electron density of the *three-coordinate* (dtbpe)Cu(NHPh) system might accelerate the nucleophilic reactivity compared with the *two-coordinate* (NHC)Cu(NHPh) systems. To test this possibility, we attempted to coordinate the Lewis base $^t$BuNC to complex **6** and probe the impact on the rate of reaction with bromoethane. The combination of **6** and $^t$BuNC reveals new resonances ($^1$H NMR spectroscopy) consistent with the formation of (IPr)Cu(NHPh)($^t$BuNC) in equilibrium with **6** and free $^t$BuNC (eq 3).

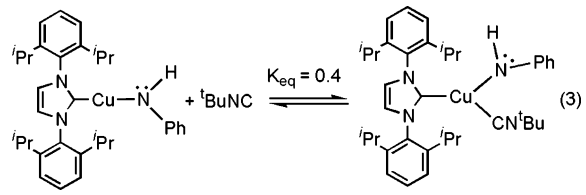


(3)

The equilibrium constant ($K_{eq}$) is 0.4 at room temperature. Even though the three-coordinate complex (IPr)Cu(NHPh)-($CN^tBu$) is not isolable, the rate of the reaction with bromoethane was determined to discern if the coordination of the isonitrile influences the rate of reaction. The kinetic studies of **6** and bromoethane in the presence of 2 equiv of $^t$BuNC (relative to [**6**]) reveal $k_{obs} = 2.36(9) \times 10^{-4}$ $s^{-1}$, which is within the standard deviation of the rate observed for **6** and bromoethane in the absence of $^t$BuNC. Therefore, weak binding of $^t$BuNC does not result in enhanced reactivity of **6** with bromoethane.

**Comparison of Calculated Electronic Structures of $Cu^I$ Anilido Complexes.** Geometry optimizations of full experimental models were carried out at the B3LYP/6-31G(d) level of theory for the $Cu^I$ anilido complexes (dtbpe)Cu(NHPh), (IPr)Cu(NHPh) (**6**), (SIPr)Cu(NHPh) (**9**), and (IMes)Cu-(NHPh) (**12**). For the dtbpe (two molecules in the asymmetric unit), IPr, and SIPr complexes, direct comparison of theory and experiment are possible (calculated values are given first with experimental values in parentheses). (IPr)Cu(NHPh) (**6**): Cu−N = 1.822 Å (1.841 Å), $Cu-C_{NHC}$ = 1.835 Å (1.875 Å), $N-Cu-C_{NHC}$ = 179.2° (174.8°), $Cu-N-C_{ipso}$ = 126.8° (127.5°). (SIPr)Cu(NHPh) (**12**): Cu−N = 1.818 Å (1.846 Å), $Cu-C_{NHC}$ = 1.833 Å (1.876 Å), $N-Cu-C_{NHC}$ = 178.5° (175.2°), $Cu-N-C_{ipso}$ = 124.6° (127.9°). (dtbpe)-Cu(NHPh): Cu−N = 1.872 Å (1.890 Å, 1.898 Å), Cu−P = 2.224 and 2.249 Å (2.249−2.298 Å), P−Cu−P = 95.8° (93.2 and 93.6°), P−Cu−N = 140.9 and 122.9° (141.0 and 125.6°, 143.3 and 123.0°), $Cu-N-C_{ipso}$ = 135.4° (134.6 and 133.3°). The comparative data reveal good agreement between the calculated and experimental bond lengths and bond angles.

At the obtained minima, pertinent molecular and electronic structural parameters were calculated at the same B3LYP/6-31G(d) level of theory, and these data are organized in Table 5. As anticipated, it is apparent that the *N*-heterocyclic carbene complexes are more similar to each other and thus distinct from the bulky, chelating bisphosphine complex (dtbpe)Cu(NHPh). The Cu−N bond is longer by ~0.05 Å for the dtbpe complex than for the NHC derivatives, commensurate with the experimentally measured bond length differences. The calculated $Cu-N_{amido}$ bond energies are ~7 kcal/mol stronger for the NHC complexes than for (dtbpe)-Cu(NHPh), regardless of the geometries of the bond-dissociation products (anilido radical and LCu) being allowed to relax (the bond-dissociation enthalpies) or not (the so-called "snap" bond energies). The calculated BDEs (Cu−

**Chart 2.** Order of Reaction Rate for the Conversion of Anilido Complexes and Bromoethane to the Metal−Bromide and Ethylaniline

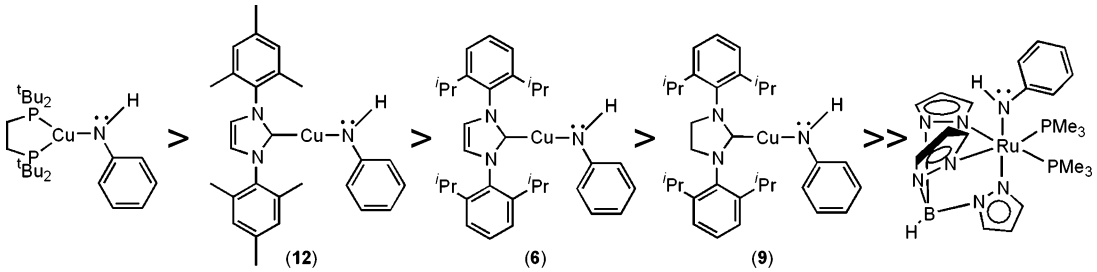


**Table 5.** Calculated Molecular and Electronic Structural Properties of $Cu^{I}$−Anilido Complexes[a]

| | Cu−N (Å) | Cu···$H_{\alpha}$[b] (Å) | Cu−N−$C_{ipso}$ (deg) | $\epsilon_{HOKSO}$[c] (eV) | $\epsilon_{LUKSO}$[c] (eV) | $q_N$[d] (au) | $q_{Cu}$[d] (au) |
|---|---|---|---|---|---|---|---|
| IPr | 1.822 | 2.509 | 126.8 | −3.62 | −0.55 | −0.82 | 0.25 |
| IMes | 1.815 | 2.519 | 124.8 | −3.61 | −0.60 | −0.84 | 0.25 |
| SIPr | 1.818 | 2.522 | 123.2 | −3.68 | −0.45 | −0.83 | 0.25 |
| dtbpe | 1.872 | 2.485 | 135.4 | −3.64 | −0.14 | −0.80 | 0.05 |

[a] Properties calculated at optimized geometries for full ligand models at the B3LYP/6-31G(d) level of theory. [b] Distance (Å) from copper to proton attached to anilido nitrogen. [c] Energies (eV) of the highest-occupied and lowest-unoccupied Kohn−Sham orbitals, KS-HOMO and KS-LUMO, respectively. [d] Mulliken atomic charges at the anilido nitrogen and copper.

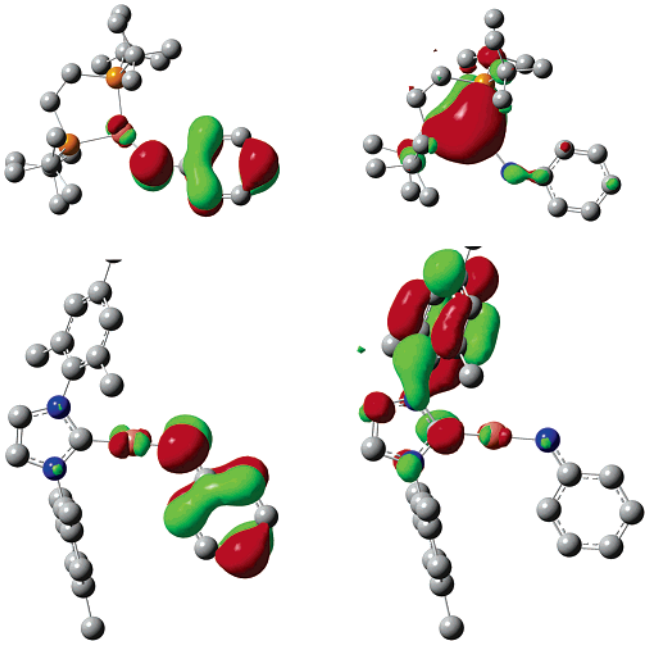

**Figure 8.** Highest-occupied (left) and lowest-unoccupied (right) Kohn−Sham orbitals for (dtbpe)Cu(NHPh) (top pair) and (IMes)Cu(NHPh) (bottom pair). The orbitals for other NHC $Cu^{I}$ anilido complexes are similar.

$N_{amido}$) are substantial at 87.3 (IPr), 88.3 (IMes), 86.7 (SIPr), and 81.8 kcal/mol (dtbpe).

While the calculated atomic charges always possess some degree of uncertainty, particularly for transition metal complexes, the similarity of the systems being studied provides confidence that the values are reasonable, if not in magnitude then in direction. All $Cu^{I}$ complexes possess a negative charge at the anilido nitrogen, which implies nucleophilic character at this site, with the dtbpe complex being slightly less negative than the NHC counterparts. Additionally, the Cu is calculated to have a positive charge of +0.25 for the NHC complexes and +0.05 for (dtbpe)-Cu(NHPh). The copper charges suggest that the metal will be less acidic/electrophilic for the dtbpe complex versus the NHC derivatives, a conjecture supported by the calculation of the energy of the lowest-unoccupied Kohn−Sham orbital (KS-LUMO), which is higher by ∼0.4 eV for the dtbpe complex. However, caution is appropriate for the latter point as the KS-LUMO is a Cu-based orbital for the dtbpe complex, while the KS-LUMOs possess primarily ligand-based character for the NHC complexes (see Figure 8). There is more uniformity in the orbital composition of the KS-HOMOs, with the DFT calculations indicating that most of the orbital composition is on the anilido ligand. There is minimal copper character to the KS-HOMOs, and that which is found appears to be Cu 3d rather than Cu 4p. Thus, analysis of DFT calculations reveal the KS-HOMOs to be primarily an anilido p$\pi$-orbital with slight $\pi$*-character from a Cu d$\pi$-orbital.* These results are consistent with the lack of evidence of hindered Cu−$N_{anilido}$ bond rotation at temperatures down to −80 °C experimental, which may also suggest negligible anilido to Cu-4p $\pi$-donation for these complexes. The artificial construction of a $C_s$ symmetric structure in which the anilido ligand is perpendicular to the NHC ring to mimic a plausible transition state for Cu−N rotation yields a stationary point that is only 1 kcal/mol higher in enthalpy, suggesting a relatively low barrier for torsion about this bond. In all cases, the KS-HOMOs have $\pi$-delocalization among the anilido nitrogen and the carbons that compose the phenyl ring. This interaction is presumably sufficient in strength to keep the anilido nitrogen planar. The calculation for rotation about the $N_{anilido}$−$C_{ipso}$ bond reveals an enthalpy of activation of 11 kcal/mol, which is similar to the experimentally determined value of 7 kcal/mol (see above).

**Experimental and Computational Study of Reactions of (IPr)Cu(NHPh) (6) and Benzene or Dihydrogen.** (IPr)-Cu(NHPh) (**6**) was separately heated (80 °C) in $C_6H_6$ and $C_6D_6$ for 24 h with no reaction. Conversely, (IPr)Cu(Ph) (**4**) reacts with aniline in $C_6D_6$ to form **6** and benzene (eq 4).

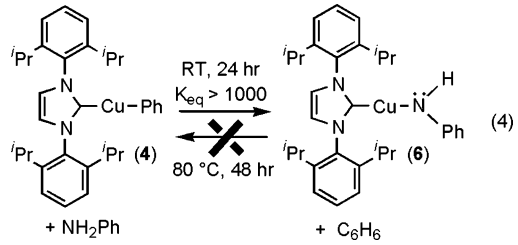


Phenyl complex **4** is completely consumed at room temper-

**Scheme 5.** DFT Calculated Changes in Enthalpy for Conversion of Transition Metal Hydride Complexes and Aniline to Transition Metal Anilido Complexes and Dihydrogen

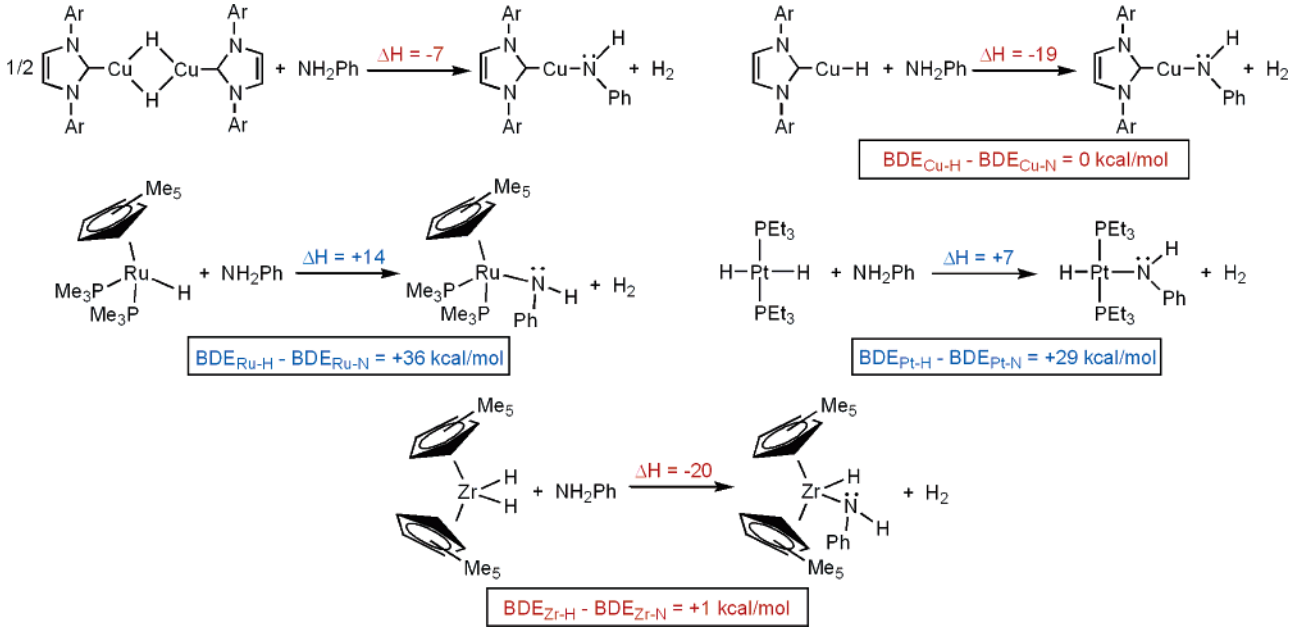


ature after 24 h. If it is assumed that 5% of **4** (relative to **6**) can be detected by $^1$H NMR spectroscopy, the $K_{eq}$ is greater than 1000 for the equilibrium between **4**/aniline and **6**/benzene.

When complex **6** is placed under 60 psi of dihydrogen in benzene at ambient temperature, no reaction occurs after 18 h. The anilido complex persists, and neither aniline nor the previously reported Cu$^I$ hydride complex [(IPr)Cu($\mu$-H)]$_2$ is produced.[42] To determine if the kinetics or thermodynamics is responsible for the lack of reaction between **6** and dihydrogen, [(IPr)Cu($\mu$-H)]$_2$ was synthesized according to the procedure reported by Sadighi et al.[6] The reaction of [(IPr)Cu($\mu$-H)]$_2$ with aniline rapidly produces gas (presumably $H_2$) and complex **6** at room temperature, as confirmed by $^1$H NMR spectroscopy (eq 5).

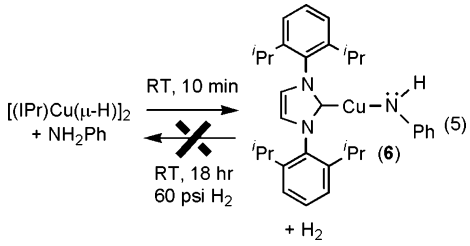


It has been noted that the thermodynamics of reactions between transition metal amido complexes and dihydrogen to form metal hydride complexes and free amine are dependent upon the identity of the metal center.[12] Early transition metal systems tend to favor transition metal amido/free dihydrogen, while late transition metal complexes exhibit a predilection toward transition metal hydride/free amine formation. This trend has been rationalized by increased metal−amido bond energies resulting from the efficient amido-to-metal $\pi$-bonding for early transition metal systems versus late transition metal complexes, for which $\pi$-bonding is often disrupted (see above).[12,55] Examples of systems that follow these trends include the conversion of Cp*Ru(PMe$_3$)$_2$(NPh$_2$) (Cp* = pentamethylcyclopentadienyl) and dihydrogen to produce free amine and Ru hydride complexes,[56] reaction of (PCP)Ru(CO)(NH$_2$) (PCP = $\eta^3$-C$_6$H$_3$-2,6-(CH$_2$P$^t$Bu$_2$)$_2$) and dihydrogen to produce free ammonia and Ru hydride complexes,[5] the release of aniline and formation of a Pt dihydride upon combination of *trans*-(PEt$_3$)$_2$Pt(H)NHPh and dihydrogen,[57] and the reaction of Cp*$_2$M(H)$_2$ (M = Zr or Hf) with ammonia to produce dihydrogen and the corresponding parent amido complexes.[56] Interestingly, despite evidence that the amido-to-Cu $\pi$-interaction is negligible or weak (see above), the conversion of [(IPr)Cu($\mu$-H)]$_2$ and aniline to (IPr)Cu(NHPh) (**6**) and dihydrogen is consistent with the reactivity of early transition metal complexes.[58] The conversion of (IPr)Cu(Ph) (**4**) and aniline to (IPr)Cu(NHPh) (**6**) and benzene also contrasts to reactivity observed with another late transition metal anilido complex. (PCP)Ir(H)(Ph) and free NH$_2$Ph are thermally favored over (PCP)Ir(H)(NHPh) and free C$_6$H$_6$ with $K_{eq}$ = 105.[59] Thus, the (IPr)Cu$^I$ fragment demonstrates a thermodynamic propensity for the formation of a Cu−NHPh bond that is atypical of late transition metal systems, which seems to suggest a shift in the relative magnitude of the M−H/M−N$_{anilido}$ and M−C$_{phenyl}$/M−N$_{anilido}$ BDEs from established norms. To probe these results in more details, we used computational studies for equilibria between metal−hydride/aniline and metal−anilido/dihydrogen for four systems (Scheme 5).

(55) Connor, J. A. *Topics Curr. Chem.* **1977**, *71*, 71−110.
(56) Bryndza, H. E.; Fong, L. K.; Paciello, R. A.; Tam, W.; Bercaw, J. E. *J. Am. Chem. Soc.* **1987**, *109*, 1444−1456.
(57) Cowan, R. L.; Trogler, W. C. *J. Am. Chem. Soc.* **1989**, *111*, 4750−4761.
(58) Hillhouse, G. L.; Bercaw, J. E. *J. Am. Chem. Soc.* **1984**, *106*, 5472−5478.
(59) Kanzelberger, M.; Zhang, X.; Emge, T. J.; Goldman, A. S.; Zhao, J.; Incarvito, C.; Hartwig, J. F. *J. Am. Chem. Soc.* **2003**, *125*, 13644−13645.

The experimental BDE of dihydrogen is 104 kcal/mol and the N−H BDE of aniline is 92 kcal/mol,[60] and thus, ignoring entropic contributions, if the resulting M−H bond is > 12 kcal/mol stronger than the $M-N_{amido}$ bond, then the equilibrium will favor the transition metal hydride/amine side of the reaction. Calculations at the B3LYP/6-31G(d) level of theory reveal a difference in the BDE values of dihydrogen and aniline (N−H) of ∼20 kcal/mol. For the equilibrium between putative monomeric complex (IPr)Cu(H) and free aniline with complex **6** and free dihydrogen, these calculations reveal that $\Delta H = -19.3$ kcal/mol with $\Delta G = -17.9$ kcal/mol (Scheme 5). If the dimerization energy for $[(IPr)Cu(\mu\text{-}H)]_2$ (i.e., net reaction is 0.5 equiv of the Cu dimer and aniline converted to 1 equiv of **6** and dihydrogen) is taken into account, the reaction is less exothermic and exergonic but still favorable: $\Delta H = -6.8$ kcal/mol and $\Delta G = -9.3$ kcal/mol.

A series of B3LYP/CEP-31G(d) calculations of M−H/free aniline and M−NHPh/free dihydrogen equilibria for representative early transition metal, late transition metal, and (NHC)Cu models was performed (Scheme 5). The choice of an effective core potential approach [CEP-31G(d)] is necessitated by the heavy metals Zr, Ru, and Pt. Calculations reproduce the experimental observations [i.e., (NHC)Cu hydrides (monomer and dimer) favor the anilido complex as does the early high-valent metal complex $Cp_2ZrH_2$]. The later low-valent Ru and Pt complexes favor the hydride side of the equilibrium.

Analysis of the metal−anilido and metal−hydride BDEs is instructive, although these values should be viewed as approximate given the small hydrogen basis sets being used. For the Pt and Ru complexes, the calculated BDEs(M−anilido) are substantially weaker than the corresponding BDEs(M−H): BDE(Pt−H) = 72 kcal/mol, BDE(Pt−anilido) = 43 kcal/mol, BDE(Ru−H) = 71 kcal/mol, and BDE(Ru−anilido) = 35 kcal/mol. Hence, the considerably stronger M−H bond versus the $M-N_{anilido}$ bond countermands the thermodynamic preference for $H_2$ versus aniline. For Zr and Cu, the M−H and $M-N_{anilido}$ bond strengths are comparable, thus pushing the equilibrium to the right given the 12 kcal/mol (experimental) advantage for BDE(H−H) over BDE(aniline N−H): BDE(Zr−H) = 68 kcal/mol, BDE(Zr-anilido) = 67 kcal/mol, and BDE{monomeric (IPr)Cu−H} = BDE{$(IPr)Cu-N_{anilido}$} = 87 kcal/mol. The calculated BDE(M−H) values show much less variance than the BDE(M−anilido) values, implying that it is primarily differences in the latter that dictate the course of the aniline/$H_2$ equilibrium. The difference in $M-N_{anilido}$ BDEs between Ru, Pt, and Zr can be rationalized by relatively strong anilido-to-Zr $\pi$-bonding with such a $\pi$-bonding interaction nonexistent or negligible for Ru and Pt. Octahedral $Ru^{II}$ has no vacant orbital of $\pi$-symmetry and $Pt^{II}$ only offers a relatively high-energy p$\pi$-orbital. Consistent with the differences in $\pi$-bonding interactions between $Zr^{IV}$, $Pt^{II}$, and $Ru^{II}$, calculations reveal that the Ru and Pt anilido complexes display significant pyramidal character at the anilido nitrogen, while the Zr complex is planar at the anilido nitrogen. The calculated Cu complexes also display a planar anilido ligand; however, similar to $Pt^{II}$, the only vacant Cu-based atomic orbital of $\pi$-symmetry is a relatively high-energy 4p orbital, and both computational results suggest negligible amido-to-Cu $\pi$-donation. Thus, the strong Cu−anilido bond is difficult to rationalize using traditional considerations.

Natural bond-orbital (NBO) calculations show the anilido nitrogen in the Pt and Ru complexes to be $sp^3$ hybridized, consistent with the pyramidal geometry at this atom.[61] The calculations reveal that the anilido nitrogen atoms in the Zr and Cu complexes are planar, which *may* arise, in part, from the $\pi$-interaction between the anilido N and the phenyl substituent rather than anilido-to-metal $\pi$-donation, as expected for earlier high-valent metal complexes such as $Zr^{IV}$. Although the arguments about hybridization based on planarity versus pyramidal character for amido ligands are tenuous (e.g., Grotjahn et al. have reported a gas-phase structural analysis of $LiNH_2$ that suggests a planar nitrogen),[62] the fact that geometry optimization of an $(NHC)Cu(NH_2)$ model yields a pyramidal amido nitrogen suggests that the phenyl ring may play a role in the planarity of the anilido nitrogen and, hence, suggest $sp^2$ hybridization. While the Zr orbital used for the bond to the anilido nitrogen is primarily d in nature, Cu uses an orbital that is predominantly 4s (89% s and 10% d by the NBO analysis). Combining the various pieces of evidence, we suggest the possibility that the combination of an $sp^2$-hybridized anilido nitrogen with the larger 4s orbital used for bonding by Cu may result in better metal−anilido $\sigma$-overlap, which would result in relatively strong $Cu-N_{anilido}$ bonds. It is also likely that the low-coordination number enforced by the bulky NHC ligands also enhances copper−anilido bonding.

## Conclusions

Monomeric copper(I) methyl complexes that possess the *N*-heterocyclic carbene ligands IPr, SIPr, and IMes react with aniline, ethanol, or phenol to release methane and form the corresponding copper(I) anilido, ethoxide, and phenoxide complexes, and the solid-state structures have confirmed the monomeric nature of these complexes. The $(NHC)Cu^I$ methyl, phenyl, and anilido complexes are quite stable under an inert atmosphere. The methyl complexes do not decompose until they are heated (in $C_6D_6$) to temperatures between 100 and 130 °C. The $Cu^I$ phenyl systems decompose between 120 and 130 °C, and (IPr)Cu(NHPh) is stable for prolonged periods of time in $C_6D_6$ at temperatures up to 130 °C. The stability of these systems is likely attributable, at least in part, to the substantial BDEs (calculated) of ∼80 kcal/mol for the Cu−Me bond, ∼95 kcal/mol for the Cu−Ph bond, and ∼87 kcal/mol for the $Cu-N_{anilido}$ bond.

(60) Luo, Y.-R. *Handbook of Bond Dissociation Energies in Organic Compounds*; CRC Press: Boca Raton, FL, 2003.

(61) Weinhold, F.; Landis, C. R. *Chem. Educ.: Res. Pract. Eur.* **2001**, *2*, 91−104.

(62) Grotjahn, D. B.; Sheridan, P. M.; Al Jihad, I.; Ziurys, L. M. *J. Am. Chem. Soc.* **2001**, *123*, 5489−5494.

(63) Cope, A. C. *J. Am. Chem. Soc.* **1935**, *57*, 2238−2240.

(64) Arduengo, A. J., III; Krafczyk, R.; Schmutzler, R.; Craig, H. A.; Goerlich, J. R.; Marshall, W. J.; Unverzagt, M. *Tetrahedron* **1999**, *55*, 14523−14534.

For reaction with bromoethane, which resembles a traditional $S_N2$ transformation, the $Cu^I$ anilido complexes have been shown to undergo reaction more rapidly than a related $Ru^{II}$ anilido complex, and relative kinetics are consistent with increasing nucleophilicity in the order $TpRu(PMe_3)_2(NHPh) \ll (SIPr)Cu(NHPh) < (IPr)Cu(NHPh) < (IMes)Cu(NHPh) < (dtbpe)Cu(NHPh)$. Given that the $Ru^{II}$ amido complexes are among the most reactive (i.e., nucleophilic and basic) transition metal amido complexes, the enhanced reactivity of the Cu systems compared to Ru suggests that the Cu complexes might be exploited for a variety of metal-mediated synthetic processes. Highly nucleophilic reactivity is a common feature of amido ligands coordinated to late transition metals in low oxidation states.

(IPr)Cu(NHPh)/free dihydrogen and (IPr)Cu(NHPh)/free benzene are thermodynamically favored over $(IPr)Cu(\mu\text{-}H)]_2$/free $NH_2Ph$ and (IPr)Cu(Ph)/free $NH_2Ph$, respectively, which is in contrast to previously observed reactivity patterns of late transition metal amido systems and is consistent with early transition metal systems. Thus, the $Cu^I$−anilido complexes exhibit an interesting mixture of features consistent with both early (likely based on the homolytically strong Cu−X bonds) and late (likely based on weak Cu−X $\pi$-interaction) transition metal complexes. Calculations suggest that the origin of the thermodynamic preferences is an unusually strong $M-N_{anilido}$ BDE. It should be noted that the (dtbpe)Cu(NHPh) and (NHC)Cu(NHPh) are, to our knowledge, the only examples of isolable monomeric $Cu^I$ amido complexes, and perhaps the calculated large $Cu-N_{anilido}$ BDEs are a hallmark of this class of complexes. Although the source of the apparently large $Cu-N_{anilido}$ BDE is not definitively known, the involvement of the Cu 4s orbital in Cu−N $\sigma$-bonding, possible $sp^2$ hybridization of the anilido nitrogen, and low coordination number of the Cu systems may contribute.

## Experimental Section

**General Methods.** All procedures were performed in a glovebox under an inert atmosphere of dinitrogen or using standard Schlenk techniques. The glovebox atmosphere was maintained by periodic nitrogen purges and monitored by an oxygen analyzer {$O_2$ (g) < 15 ppm for all reactions}. Benzene, toluene, THF, and hexanes were purified by reflux over sodium, followed by distillation. Benzene-$d_6$ and toluene-$d_8$ were distilled over sodium, degassed by three freeze−pump−thaw cycles, and stored over 4 Å molecular sieves. $CDCl_3$ was distilled over calcium hydride, degassed by three freeze−pump−thaw cycles, and stored over 4 Å molecular sieves. All reactions performed on an NMR scale used J-Young NMR tubes that were loaded in a glovebox. $^1H$ and $^{13}C$ NMR measurements were performed on either a Varian Mercury 400 MHz or a Varian Mercury 300 MHz spectrometer (operating frequencies for $^{13}C$ NMR spectra were 100 and 75 MHz, respectively) and referenced to TMS using resonances from residual protons in the deuterated solvents or the $^{13}C$ resonances of the deuterated solvents. IR spectra were obtained on a Mattson Genesis II spectrometer either as thin films on a KBr plate or in solution using a KBr solution cell. Electrochemical experiments were performed under a nitrogen atmosphere using a BAS Epsilon potentiostat. Cyclic voltammograms were recorded in a standard three-electrode cell from −2.00 to +2.00 V with a glassy carbon working electrode and tetrabutylammonium hexafluorophosphate as the electrolyte. Tetrabutylammonium hexafluorophosphate was dried under dynamic vacuum at 140 °C for 48 h prior to use. All potentials are reported versus NHE (normal hydrogen electrode) using cobaltocenium hexafluorophosphate as an internal standard. Copper(I) chloride, TEMPO, MeLi, and 1,4-cyclohexadiene were obtained from commercial sources and used as received. Copper(I) acetate was purchased from Strem Chemical and used as received. Diphenylmagnesium was prepared according to a reported procedure.[63] The ligands SIPr and IMes were prepared according to reported procedures.[64] The synthesis and characterization of (IPr)Cu(NHPh) (**6**), (IPr)Cu(OEt) (**7**), and (IPr)Cu(OPh) (**8**) have been reported in a preliminary communication.[46] The copper complexes (IPr)Cu(Cl), (IPr)Cu(OAc), (IPr)Cu(Me) (**1**), $[(IPr)Cu(\mu\text{-}H)]_2$, (SIPr)Cu(Me) (**2**), and (IMes)Cu(Me) (**3**) were prepared according to reported procedures.[41,42,46,48] Synthetic and characterization details of (SIPr)Cu(Cl), (IMes)Cu(Cl), (IMes)Cu(Me), and (IPr)Cu(Br) are available in the Supporting Information.

**(IPr)Cu(Ph) (4).** Five mL of benzene was added to a round-bottom flask charged with (IPr)Cu(Cl) (0.100 g, 0.19 mmol) and diphenylmagnesium (0.056 g, 0.31 mmol). The pale yellow solution was stirred for 1 h, after which it was filtered through a plug of Celite. The solvent volume was reduced by approximately half in vacuo, and hexanes were added to yield a cream precipitate. The solid was collected by vacuum filtration and dried (0.072 g, 64%). NMR ($C_6D_6$): $\delta$ 7.65 (d, $J = 6$ Hz, 2H, *o*-Ph), 7.23 (br t, $J = 7$ Hz, 3H, overlap of *p*-aryl of IPr and Ph), 7.08 (br d, $J = 7$ Hz, 3H, overlap of *m*-aryl of IPr and Ph), 6.30 (s, 2H, NC*H*), 2.66 (sept, $J = 6$ Hz, 4H, C*H*$(CH_3)_2$), 1.43 (d, $J = 6$ Hz, 12H, CH(C*H*$_3)_2$), 1.12 (d, $J = 6$ Hz, 12H, CH(C*H*$_3)_2$). $^{13}C$ NMR ($C_6D_6$): $\delta$ 186.2 (N*C*Cu), 166.0, 146.2, 141.1, 135.8, 128.9, 126.6, 124.7, 124.6, 122.7 (aryl of IPr, phenyl and N*C*H), 29.6 (*C*H$(CH_3)_2$), 25.7 (CH(*C*H$_3)_2$), 24.2 (CH(*C*H$_3)_2$). We were unable to obtain satisfactory elemental analysis of this complex. The $^1H$ NMR spectrum is provided in the Supporting Information.

**(SIPr)Cu(Ph) (5).** Five mL of THF was added to a round-bottom flask charged with (SIPr)Cu(Cl) (0.130 g, 0.31 mmol) and diphenylmagnesium (0.100 g, 0.40 mmol). The pale yellow solution was stirred for 18 h and was then filtered through Celite. The solvent volume was reduced by approximately half in vacuo, and hexanes were added to yield a tan solid. The solid was collected by vacuum filtration and dried (0.080 g, 49%). The $^1H$ NMR spectrum reveals resonances consistent with **5** plus ~20% of an intractable impurity. $^1H$ NMR ($C_6D_6$): $\delta$ 7.55 (d, $J = 7$ Hz, 2H, *o*-Ph), 7.20 (t, $J = 8$ Hz, 2H, *p*-aryl of SIPr), 7.08 (d, $J = 7$ Hz, 4H, *m*-aryl of SIPr), 3.17 (s, 4H, NC*H*), 3.04 (sept, $J = 7$ Hz, 4H, C*H*$(CH_3)_2$), 1.49 (d, $J = 7$ Hz, 12H, CH(C*H*$_3)_2$), 1.20 (d, $J = 7$ Hz, 12H, CH(C*H*$_3)_2$). The meta and para protons on the phenyl group are coincidental with the solvent and SIPr aryl peaks. $^{13}C$ NMR ($C_6D_6$): $\delta$ 207.7 (N*C*Cu), 165.4, 147.0, 140.7, 135.4, 130.1, 129.8, 126.3, 116.5, 124.7, 124.6, 124.4 (phenyl on SIPr ligand and phenyl), 53.4 (N*C*H), 29.2 (*C*H$(CH_3)_2$), 25.7 (CH(*C*H$_3)_2$), 23.8 (CH(*C*H$_3)_2$). The $^1H$ NMR spectrum is provided in the Supporting Information.

**(SIPr)Cu(NHPh) (9). Method A.** (SIPr)Cu(Me) (0.080 g, 0.17 mmol), benzene (5 mL), and aniline (16 $\mu$L, 0.17 mmol) were added sequentially to a thick-walled glass pressure tube. The solution was heated for 48 h at 60 °C. The solution was cooled to room temperature, the volume reduced approximately by half in vacuo, and hexanes were added to yield a white solid. The solid was collected and dried (0.060 g, 65%). **Method B.** (SIPr)Cu(Cl) (0.144 g, 0.29 mmol) was dissolved in benzene (10 mL), and LiNHPh (0.0276 g, 0.28 mmol) was added. The pale yellow solution was stirred for 2 h and then filtered through Celite. The benzene volume

was reduced by approximately half in vacuo, and hexanes were added to yield a pale yellow solid (0.0934 g, 61%). Crystals suitable for a solid-state X-ray diffraction study were grown at room temperature by layering a toluene solution of **9** with pentane. $^1$H NMR ($C_6D_6$): $\delta$ 7.27 (t, $J$ = 8 Hz, 2H, *p*-aryl of SIPr), 7.11 (d, $J$ = 8 Hz, 4H, *m*-aryl of SIPr), 6.97 (t, $J$ = 7 Hz, 2H, *m*-phenyl of NHPh), 6.49 (t, $J$ = 7 Hz, 1H, *p*-phenyl of NHPh), 5.88 (d, $J$ = 7 Hz, 2H, *o*-phenyl of NHPh), 3.17 (s, 4H, NC*H*), 3.12 (br s, 1H, N*H*), 2.98 (sept, $J$ = 7 Hz, 4H, C*H*($CH_3$)$_2$), 1.42 (d, $J$ = 7 Hz, 12H, CH(C*H*$_3$)$_2$), 1.18 (d, $J$ = 7 Hz, 12H, CH(C*H*$_3$)$_2$). $^{13}$C NMR ($C_6D_6$): $\delta$ 204.7 (N*C*Cu), 161.4, 147.9, 135.9, 130.6, 129.7, 125.4, 116.8, 111.1, 100.9 (SIPr aryl, anilido phenyl), 54.0 (N*C*H), 29.8 (*C*H(CH$_3$)$_2$), 26.2 (CH(*C*H$_3$)$_2$), 24.6 (CH(*C*H$_3$)$_2$). We were unable to obtain a satisfactory elemental analysis of this complex. The $^1$H spectrum is provided in the Supporting Information.

**(SIPr)Cu(OEt) (10).** Ethanol (9 $\mu$L, 0.16 mmol) was added to a pressure tube charged with (SIPr)Cu(Me) (0.075 g, 0.16 mmol) and 4 mL of benzene. The solution was heated for 1 h at 60 °C. The solution volume was reduced approximately by half in vacuo, and hexanes were added to yield a white solid. The solid was collected by vacuum filtration and dried (0.076 g, 72%). Crystals were grown by layering a concentrated benzene solution of **10** with pentane. $^1$H NMR ($C_6D_6$): $\delta$ 7.21 (t, $J$ = 8 Hz, 2H, *p*-aryl of SIPr), 7.07 (d, $J$ = 8 Hz, 4H, *m*-aryl of SIPr), 4.24 (q, $J$ = 7 Hz, 2H, OC*H*$_2$CH$_3$), 3.20 (s, 4H, NC*H*), 2.99 (sept, $J$ = 7 Hz, 4H, C*H*($CH_3$)$_2$), 1.47 (d, $J$ = 6 Hz, 12H, CH(C*H*$_3$)$_2$), 1.19 (d, $J$ = 7 Hz, 12H, CH(C*H*$_3$)$_2$), 1.08 (t, $J$ = 7 Hz, 3H, OCH$_2$C*H*$_3$). $^{13}$C NMR ($C_6D_6$): $\delta$ 205.0 (N*C*Cu), 147.3, 135.9, 130.1, 126.9, 125.0 (aryl of SIPr), 53.7 (N*C*H), 29.4 (*C*H(CH$_3$)$_2$), 25.9 (CH(*C*H$_3$)$_2$), 24.3 (CH(*C*H$_3$)$_2$). Resonances from Cu-O*C*H$_2$CH$_3$ were not observed. We were unable to obtain a satisfactory elemental analysis of this complex. The $^1$H NMR spectrum is provided in the Supporting Information.

**(SIPr)Cu(OPh) (11).** Phenol (0.015 g, 0.16 mmol) was added to a round-bottom flask charged with (SIPr)Cu(Me) (0.075 g, 0.16 mmol) and 4 mL of benzene. Evolution of a gas (presumably methane) was immediately observed. The benzene volume was reduced by approximately half in vacuo, and hexanes were added to yield a white solid. The solid was collected by vacuum filtration and dried (0.075 g, 86%). Crystals were grown by layering a concentrated toluene solution of **11** with pentane. $^1$H NMR ($C_6D_6$): $\delta$ 7.25 (t, $J$ = 8 Hz, 2H, *p*-aryl of SIPr), 7.12−7.07 (overlapping multiplets, 6H, *m*-OPh and *m*-aryl of SIPr), 6.68 (t, $J$ = 7 Hz, 1H, *p*-OPh), 6.38 (d, $J$ = 8 Hz, 2H, *o*-OPh), 3.15 (s, 4H, NC*H*), 2.93 (sept, $J$ = 7 Hz, 4H, C*H*($CH_3$)$_2$), 1.35 (d, $J$ = 7 Hz, 12H, CH(C*H*$_3$)$_2$), 1.16 (d, $J$ = 7 Hz, 12H, CH(C*H*$_3$)$_2$). $^{13}$C NMR ($C_6D_6$): $\delta$ 205.2 (N*C*Cu), 147.6, 135.7, 130.8, 129.8, 125.5, 120.9 114.3, 112.5 (aryl of SIPr and OPh), 54.0 (N*C*H), 29.8 (*C*H(CH$_3$)$_2$), 26.2 (CH(*C*H$_3$)$_2$), 24.5 (CH(*C*H$_3$)$_2$). One resonance from the aryl rings was not observed presumably because of coincidental overlap. Anal. Calcd for $C_{33}H_{43}CuN_2O$: C, 72.43; H, 7.92; N, 5.12. Found: C, 72.18; H, 7.81; N, 5.05.

**(IMes)Cu(NHPh) (12).** A round-bottom flask was charged with (IMes)Cu(Cl) (0.050 g, 0.12 mmol) and 5 mL of benzene, and LiNHPh (0.012 g, 0.12 mmol) was added to the solution. The pale yellow solution was stirred for 4 h and then filtered through Celite. The solvent volume was reduced by approximately half in vacuo, and hexanes were added to yield a pale yellow precipitate. The solid was collected by vacuum filtration and dried (0.027 g, 47%). $^1$H NMR ($C_6D_6$): $\delta$ 7.05 (t, $J$ = 7 Hz, 2H, *m*-phenyl of NHPh), 6.72 (s, 4H, *m*-aryl of IMes), 6.55 (t, $J$ = 7 Hz, 1H, *p*-phenyl of NHPh), 6.25 (d, $J$ = 7 Hz, 2H, *o*-phenyl of NHPh) 5.97 (s, 2H, NC*H*), 3.38 (bs, 1H, N*H*), 2.13 (s, 6H, *p*-CH$_3$), 1.95 (s, 12H, *o*-C*H*$_3$). $^{13}$C NMR ($C_6D_6$): $\delta$ 181.8 (N*C*Cu), 161.2 (CuN*C*), 139.3, 135.9, 134.9, 129.6, 129.0, 121.4, 116.3, 110.4 (aryl of IMes and anilido ligands and N*C*H), 21.3 (*p*-*C*H$_3$), 17.9 (*o*-*C*H$_3$). We were unable to obtain a satisfactory elemental analysis of this complex. The $^1$H NMR spectrum is provided in the Supporting Information.

**(IMes)Cu(OEt) (13).** Ethanol (16 $\mu$L, 0.28 mmol) was added to a pressure tube charged with (IMes)Cu(Me) (**3**) (0.075 g, 0.20 mmol) and 10 mL of benzene. The solution was heated for 1 h at 60 °C. A 0.5 mL aliquot was removed from the pressure tube, and the nonvolatiles were evaporated with a stream of dinitrogen. The residue was taken up in $C_6D_6$, and a $^1$H NMR spectrum was acquired that was consistent with the formation of (IMes)Cu(OEt) in the presence of free EtOH. At room temperature, resonances from the Cu−OEt moiety are broad, consistent with a rapid exchange (on the NMR time scale) between residual free EtOH and the Cu−OEt ligand. In contrast to the other (NHC)Cu(OEt) systems, complex **13** is apparently only stable in the presence of excess ethanol. Complete removal of EtOH, via repeated removal of nonvolatile material under reduced pressure, results in the isolation of a solid whose NMR spectra reveal multiple and intractable (NHC)Cu systems.

**(IMes)Cu(OPh) (14).** Phenol (0.021 g, 0.23 mmol) was added to a round-bottom flask charged with (IMes)Cu(Me) (0.085 g, 0.22 mmol) and 4 mL of benzene. Evolution of a gas (presumably methane) was immediately observed. After the mixture was stirred for approximately 10 min, the solvent volume was reduced by approximately half in vacuo, and hexanes were added to yield a white solid. The solid was collected by vacuum filtration and dried (0.083 g, 81%). Crystals were grown by layering a concentrated benzene solution of **14** with pentane. $^1$H NMR ($CDCl_3$): $\delta$ 6.90 (s, 2H, NC*H*), 6.85 (s, 4H, *m*-aryl of IMes), 6.64 (t, $J$ = 7.8 Hz, 2H, *m*-OPh), 6.22 (t, $J$ = 7.1 Hz, 1H, *p*-OPh), 5.90 (d, $J$ = 8.1 Hz, 2H, *o*-OPh), 2.21 (s, 6H, *p*-C*H*$_3$), 1.95 (s, 12H, *o*-C*H*$_3$). $^{13}$C NMR ($C_6D_6$): $\delta$ 181.1 (N*C*Cu), 170.5 (*ipso*-OPh), 140.1, 136.3, 135.5, 130.3, 129.9, 122.4, 121.1 (aryl of IMes and OPh), 114.4 (N*C*H), 21.9 (*p*-*C*H$_3$), 18.4 (*o*-*C*H$_3$). Anal. Calcd for $C_{27}H_{29}CuN_2O$: C, 70.33: H, 6.34: N, 6.08. Found: C, 68.92: H, 6.44: N, 5.61. The $^1$H NMR spectrum is provided in the Supporting Information.

**Thermolysis of (NHC)Cu(Me) (2) in $C_6D_6$.** A representative procedure is given. A screwcap NMR tube was charged with a solution of **2** (0.015 g, 0.032 mmol) in $C_6D_6$ (0.6 mL) and heated. The temperature ranged between 60 and 110 °C with the temperature increased in 15−20 °C intervals after 24 h of no observable transformation. After 70 h at 110 °C, complex **2** was completely consumed to form new (NHC)Cu complexes and the free organic substrates methane, ethane, and ethylene. A JEOL HX110 magnetic sector mass spectrometer (Tokyo, Japan) operating in the EI$^+$ (electron ionization) positive-ion detection mode was used to detect methane, ethane, and ethylene in the headspace of screwcap NMR tubes. The resolving power was 1000 R (90% Valley) with a source temperature of 150 °C, an ionizing voltage of 70 eV, and an accelerating voltage of 10 kV. The data were calibrated externally using PFK (perfluorokerosene) ions, and 20 $\mu$L of gas was injected for each experiment.

**Thermolysis of (SIPr)Cu(Me) (2) in the Presence of TEMPO in $C_6D_6$.** A solution of TEMPO (2,2,6,6-tetramethylpiperidinyloxy) (0.006 g, 0.038 mmol) and $C_6D_6$ (0.2 mL) was added to a J-Young tube charged with a solution of **2** (0.015 g, 0.032 mmol) in $C_6D_6$ (0.4 mL). The solution turned dark immediately. After 24 h at 130 °C, complex **2** was completely consumed to form predominantly one new copper complex and the free organics methane, ethane, and ethylene.

**Thermolysis of (SIPr)Cu(Me) (2) and 1,4-Cyclohexadiene in $C_6D_6$.** 1,4-Cyclohexadiene (6 $\mu$L, 0.064 mmol) was injected into a J-Young tube charged with a solution of **2** (0.015 g, 0.032 mmol) in $C_6D_6$ (0.6 mL). After 23 h at 130 °C, complex **2** was completely consumed to form new (NHC)Cu complexes and the free organic substrates methane, ethane, and ethylene.

**Thermolysis of (NHC)Cu(Me) (1) in Toluene-$d_8$.** A representative procedure is given. A J-Young tube was charged with a solution of **1** (0.015 g, 0.032 mmol) in toluene-$d_8$ (0.6 mL) and heated. The temperature ranged between 60 and 110 °C with the temperature increased in 15−20 °C intervals after 24 h of no observable transformation. After 70 h at 110 °C, **1** was completely consumed to form new (NHC)Cu complexes and the free organic substrates methane, ethane, and ethylene.

**Thermolysis of (NHC)Cu(Ph) (4) in $C_6D_6$.** The procedure and observations were identical for **4** and **5**. A J-Young tube was charged with a solution of **4** (0.010 g, 0.018 mmol) in $C_6D_6$ (0.6 mL) and heated at 120 °C. After 24 h, complex **4** was >95% consumed to form new (NHC)Cu complexes. Definitive identification of organic products was not possible.

**Kinetics of (NHC)Cu(NHPh) (6) and Bromoethane.** A representative procedure is given. Bromoethane (73 $\mu$L, 0.99 mmol) was added to a solution of **6** (0.045 g, 0.082 mmol) in $C_6D_6$ (2.0 mL) with hexamethylbenzene (0.0031 g, 0.019 mmol) as an internal standard. The solution was immediately divided between 3 screw-cap NMR tubes and frozen in an acetone/dry ice slush bath. The reaction mixtures were each allowed to warm to room temperature, and the conversions were followed by $^1$H NMR spectroscopy at room temperature. The integration of the peaks because of the disappearance of **6** and the appearance of ethyl aniline versus the internal standard were used to calculate the rate of the reaction using first-order plots.

**Reaction of (IPr)Cu(NHPh) (6) with *tert*-Butylisocyanide.** Complex **6** (9.4 mg, 0.017 mmol) was dissolved in toluene-$d_8$ (0.7 mL) in a J. Young NMR tube with 2 equiv of *tert*-butylisocyanide (4 $\mu$L, 0.035 mmol) and hexamethyldisiloxane (2 $\mu$L, 0.009 mmol) as an internal standard. A $^1$H NMR spectrum was taken at room temperature. Distinct new resonances appear for the alkyl peaks of the NHC ligand. The downfield methyl peak for the 2-coordinate complex has a chemical shift of 1.34 ppm,, and the new peak of the 3-coordinate complex appears at 1.44 ppm. The solution was allowed to equilibrate, and $K_{eq} = 0.4$ was determined at room temperature using the integration of the methyl peaks. Variable-temperature NMR of the solution between 25 and −75 °C demonstrated that the equilibrium is surprisingly independent of temperature.

**Kinetics of (IPr)Cu(NHPh) and Bromoethane with Added $^t$BuNC.** Complex **6** (16.1 mg, 0.030 mmol) was dissolved in $C_6D_6$ (0.73 mL) in a J-Young NMR tube with hexamethyldisiloxane (6.2 $\mu$L, 0.030 mmol) as an internal standard and 2 equiv of *tert*-butylisocyanide (6.7 $\mu$L, 0.059 mmol). Bromoethane (12 equiv, 26.3 $\mu$L, 0.35 mmol) was added by syringe, and immediately the reaction was frozen in an acetone/dry ice slush bath. The reaction was then allowed to warm to room-temperature just before the reaction was monitored at regular intervals by $^1$H NMR. The integrals of the formation of ethyl aniline and disappearance of the amido complex were recorded versus the internal standard to calculate $k_{obs} = 2.36(9) \times 10^{-4}$ s$^{-1}$, corresponding to a $t_{1/2}$ of 49.1 min.

**Reaction of (IPr)Cu(NHPh) (6) and Benzene.** A solution of **6** (0.0123 g, 0.022 mmol), $C_6H_6$ (6 $\mu$L, 0.067 mmol), and hexamethylbenzene (0.0002 g, 0.017 mmol) in $C_6D_6$ (0.7 mL) was sealed in a J-Young NMR tube and heated to 80 °C for 24 h. The reaction was monitored by $^1$H NMR periodically, and after 48 h, the NMR remained the same with no reaction and no decomposition of **6**.

**Reaction of (IPr)Cu(Ph) (4) and Aniline.** A solution of **4** (0.0165 g, 0.031 mmol) was dissolved in $C_6D_6$ (0.774 g, 9.19 mmol) with hexamethyldisiloxane (5 $\mu$L, 0.024 mmol) as an internal standard and added to a J-Young NMR tube. Aniline (3.1 $\mu$L, 0.034 mmol) was added to the tube, which was then sealed. The solution was monitored by $^1$H NMR, and complete reaction to form **6** and disappearance of **4** occurred within 24 h; $K_{eq}$, calculated on the basis of a >90% conversion, is >1000.

**Reaction of (IPr)Cu(NHPh) (6) and $H_2$.** Complex **6** (0.043 g, 0.079 mmol) was dissolved in benzene (15 mL) in a glass high-pressure tube. The tube was pressurized with $H_2$ to 60 psi for 18 h. The solution turned slightly brown. The solvent was removed from the solution in vacuo, and a $^1$H NMR spectrum ($C_6D_6$) was taken of the residue. The resonances were consistent with the starting material and a small amount of decomposition, and no resonances for [IPrCu($\mu$-H)]$_2$ were observed.

**Reaction of [(IPr)Cu($\mu$-H)]$_2$ and Aniline.** The bright yellow solid [(IPr)Cu($\mu$-H)]$_2$ (~0.01 g, 0.022 mmol) was dissolved in $C_6D_6$ and added to a J-Young NMR tube. Aniline (~0.1 mL) was added to the tube, which was then sealed. Gas evolution was observed, and the solution was colorless after 10 min. Complete reaction to form **6** and $H_2$ (4.47 ppm) and disappearance of [(IPr)Cu($\mu$-H)]$_2$ within 10 min was confirmed by $^1$H NMR by comparison with data for **6** and observations of $H_2$ in $C_6D_6$.

**Computational Methods.** All calculations were carried out with the Gaussian03 package.[65] The B3LYP functional (Becke's three-parameter hybrid functional[66] using the LYP correlation functional containing both the local and nonlocal terms of Lee, Yang, and Parr)[67] and VWN (Slater local-exchange functional[68] and the local correlation functional of Vosko, Wilk, and Nusair)[69] were employed in conjunction with the 6-31G(d) all-electron basis set, unless specified otherwise. Closed-shell (diamagnetic) and open-shell (paramagnetic) species were modeled within the restricted and unrestricted Kohn−Sham formalisms, respectively. All systems were fully optimized without symmetry constraint, and analytic calculations of the energy Hessian were performed to confirm species as minima and to obtain enthalpies in the gas phase at 1 atm and 298.15 K.

**Acknowledgment.** The Office of Basic Energy Sciences, U.S. Department of Energy (DE-FG02-03ER15490), the NSF (CAREER Award CHE 0238167), and the Alfred P. Sloan Foundation (Research Fellowship) are acknowledged for

(65) Frisch, M. J.; Trucks, G. W.; Schlegel, H. B.; Scuseria, G. E.; Robb, M. A.; Cheeseman, J. R.; Montgomery, J. A., Jr.; Vreven, T.; Kudin, K. N.; Burant, J. C.; Millam, J. M.; Iyengar, S. S.; Tomasi, J.; Barone, V.; Mennucci, B.; Cossi, M.; Scalmani, G.; Rega, N.; Petersson, G. A.; Nakatsuji, H.; Hada, M.; Ehara, M.; Toyota, K.; Fukuda, R.; Hasegawa, J.; Ishida, M.; Nakajima, T.; Honda, Y.; Kitao, O.; Nakai, H.; Klene, M.; Li, X.; Knox, J. E.; Hratchian, H. P.; Cross, J. B.; Bakken, V.; Adamo, C.; Jaramillo, J.; Gomperts, R.; Stratmann, R. E.; Yazyev, O.; Austin, A. J.; Cammi, R.; Pomelli, C.; Ochterski, J. W.; Ayala, P. Y.; Morokuma, K.; Voth, G. A.; Salvador, P.; Dannenberg, J. J.; Zakrzewski, V. G.; Dapprich, S.; Daniels, A. D.; Strain, M. C.; Farkas, O.; Malick, D. K.; Rabuck, A. D.; Raghavachari, K.; Foresman, J. B.; Ortiz, J. V.; Cui, Q.; Baboul, A. G.; Clifford, S.; Cioslowski, J.; Stefanov, B. B.; Liu, G.; Liashenko, A.; Piskorz, P.; Komaromi, I.; Martin, R. L.; Fox, D. J.; Keith, T.; Al-Laham, M. A.; Peng, C. Y.; Nanayakkara, A.; Challacombe, M.; Gill, P. M. W.; Johnson, B.; Chen, W.; Wong, M. W.; Gonzalez, C.; Pople, J. A. *Gaussian 03*, revision C.02; Gaussian, Inc.: Wallingford, CT, 2004.
(66) Becke, A. D. *J. Chem. Phys.* **1993**, *98*, 1372−1377.
(67) Lee, C.; Yang, W.; Parr, R. G. *Phys. Rev.* **1988**, *B37*, 785−789.
(68) Kohn, W.; Sham, L. *Phys. Rev.* **1965**, *140*, A1133−A1138.
(69) Vosko, S. H.; Wilk, L.; Nusair, M. *Can. J. Chem.* **1980**, *58*, 1200.

support of this research. E.D.B. acknowledges support from the American Association of University Women for an American Fellowship (Dissertation). The authors would also like to thank Professor David C. Muddiman and Mr. Matthew M. Lyndon for assistance with the mass spectrometry experiments. T.R.C. acknowledges the U.S. Department of Education for its support of the CASCaM facility. This research was supported in part by a grant from the Offices of Basic Energy Sciences, U.S. Department of Energy (Grant DEFG02-03ER15387). Calculations employed the UNT computational chemistry resource, for which T.R.C. acknowledges the NSF for support through Grant CHE-0342824.

**Supporting Information Available:** Complete data from XRD studies of complexes **9**, **10**, **11**, and **14**, kinetic plots and $^1$H NMR spectra of complexes **4**, **5**, **9**, **10**, **12**, and **14**, Cartesian coordinates for calculated structures, and experimental details for (SIPr)Cu(Cl), (IMes)Cu(Cl), (IMes)Cu(Me), and (IPr)Cu(Br). This material is available free of charge via the Internet at http://pubs.acs.org.

IC0611995